MESTRADO
MEDICINA E ONCOLOGIA MOLECULAR

Exploring the Contribution of Ovarian Ageing Hallmarks to the Development of Preneoplastic Lesions

Catarina Brandão

M

2024

Supervisor: Elisabete Silva, Ph.D.
Co-supervisors: Henrique Almeida, Ph.D.; Sara Ricardo, Ph.D.

Ageing & Stress Group, Faculty of Medicine of University of Porto
Differentiation & Cancer Group, Institute for Research and Innovation in Health

FACULDADE DE **MEDICINA**

Acknowledgements

À minha orientadora, Professora Elisabete Silva, por me ter acolhido como sua mestranda numa altura tão invulgar, mas foi graças a si, com o auxílio indispensável da Professora Sara Ricardo e Professor Henrique Almeida, meus tão cuidadosos co-orientadores, que alcancei este patamar académico onde me encontro hoje. Tenho a agradecer o apoio constante dos Professores, com os quais aprendi muito a nível laboratorial, bem como a desempenhar as minhas tarefas de modo crítico e cuidadoso. Agradeço, também, a oportunidade que me foi facultada, nestes anos de mestrado, para expandir o meu leque de conhecimento, realizando um conjunto de técnicas e apresentações que me possibilitaram evoluir como estudante e, indubitavelmente, como futura profissional. Mais ainda, de destacar o acompanhamento regular feito pelos Professores nas fases finais do trabalho, dedicando o seu tempo escasso a assegurar que tudo seria concluído impecavelmente.

À minha família, pais, irmão, avós e gatas, por me apoiarem ao longo de todo o meu percurso académico, nas suas curvas e contracurvas, por me proporcionarem as melhores oportunidades, não só educacionais como em termos familiares e de carinho, por desejarem o melhor para mim e por darem o seu melhor todos os dias, dedicando-se continuamente e esforçando-se para que nada me falte agora nem nunca, e para que todo o mundo esteja ao meu alcance. Agradeço-vos por todos os anos passados ao vosso lado, e pelas experiências que partilhámos e partilhamos em conjunto, nem que se trate de tentar encontrar novas estratégias para dar comprimidos à Mimi.

À minha namorada Filipa, que o fado trouxe até mim, que me inspira a ambicionar sempre mais, a investir em mim, que me ensina a considerar todos os pormenores em todo o meu trabalho, mesmo que não sejam determinantes, mas que se destacam aos olhos mais atentos. Grata por me acolheres de braços abertos sempre que te procuro, em absolutamente qualquer altura, nem que tenhas de improvisar uma casa para nós, enquanto sais do conforto da tua. Sou feliz com e por todos momentos que me proporcionaste ao teu lado, neste ano, que parecem ter-se sucedido numa das nossas outras vidas, tamanha a sua vastidão e multiplicidade, e que irão continuar até as nascentes deixarem de brotar água, nesta nossa narrativa épico-romântica.

À Margarida, minha melhor amiga de longa data, raio de sol de otimismo inigualável, que acompanha, pacientemente, há quase oito anos, o meu percurso, e que me apoia com unhas e dentes, mesmo perante evidências da nossa falta de razão. Constituis a claque mais invejável, a maior e melhor, e sei que, em certa medida, podíamos ser a Elena e a Lila, ou o Narciso e o Goldmundo. Obrigada pelas nossas longas conversas e trocas de cartas, que fogem do quotidiano e da repetição, e pela liberdade que sempre me deste.

Aos meus amigos da faculdade, Rita, Miguel, Laura, Laís e Rodrigo, que enriqueceram os meus anos de faculdade com a sua companhia, as suas piadas e conversas sobre tudo, os nossos passeios e férias, e os mil momentos que imortalizamos em fotografias. Através da licenciatura sombria, dos anos de pandemia, e, finalmente, do mestrado e estágio, protegeram-me da solidão, e agradeço o apoio constante, sem o qual eu não teria tido um décimo da diversão e perseverança para sair de caminhos de terra batida e enveredar por novos destinos.

Ao melhor que o voluntariado me deu, seis mulheres (e homem) inteligentes, solidários, atentos, e ferozes, que permanecem na linha da frente pelos seus soldados: Susana, Beatriz, Helena, Carolina, Inês e Francisco. Obrigada por vos ter ao meu lado, em todas as ocasiões, quer a resgatar gatos de estradas movimentadas, quer a ouvir os meus lamentos e frustrações, quer a cooperar no trabalho burocrático extenso que suportamos continuamente, quer em reencontros animados, ou na partilha do nosso amor pelos animais e pela natureza.

Aos meus colegas de laboratório, Natália, Sara e Diogo, cuja companhia foi e é imprescindível para que se tenha um bom dia de trabalho na faculdade, tanto pelas risadas constantes, como pelos gostos musicais uníssonos, que alegaram as nossas bancadas, ou pelo segundo par de olhos no trabalho realizado, sempre que foi necessário. A vossa disponibilidade constante para me acompanharem e aturarem até altas horas da noite foi uma das minhas maiores sortes neste estágio.

Table of Contents

Acknowledgements i
List of Abbreviations ix
Abstract xiv
Resumo xviii
Graphical Abstract xxii
Chapter I: State of Art 1
I.1 The Ovary 3
I.1.1 Histomorphology 3
I.1.2 Ovarian Cycle 4
I.2 Tissue Remodelling and Wound Healing in Ovulation 5
I.2.1 Wound Healing 5
I.2.2 Fibrosis 6
I.3 Inflammatory Processes in Ovulation 8
I.3.1 Innate and Adaptive Immunity and Inflammageing 8
I.3.2 Macrophage-induced Inflammatory and Oxidative Microenvironment 9
I.4 Ovarian Ageing and Cancer 11
Chapter II: Hypothesis & Aim 15
Chapter III: Materials & Methods 19
III.1 Animal Handling and Ovarian Tissue Collection 21
III.2 Tissue Processing, Fixation and Sectioning 22
III.2.1 Slide Coating 22
III.3 Staining Techniques 22
III.3.1 Haematoxylin and Eosin 23
III.3.2 Sudan Black B 23
III.4 Immunohistochemistry 24
III.5 Stained Sections Analysis and Quantification 25
III.6 Tissue Lysis 27
III.7 Protein Quantification 28
III.8 Western Blotting 28
III.9 Statistical Analysis 30
Chapter IV: Results 32
IV.1 Age-related Deposits in Ovarian Tissue 34
IV.2 Age-related Accumulation of IgG in Ovarian Tissue 35

IV.3 Evaluation of ovarian surface epithelium changes during reproductive ageing .. 38
IV.4 Fibroblast-like Stromal Cells Biomarker 39
IV.5 Influence of Parity in Ovarian Ageing 40
Chapter V: Discussion 43
Chapter VI: Conclusion and Future Perspectives 51
List of Figures & Tables 55
References 61

List of Abbreviations

Abbreviation	Definition	Page
α-SMA	α-smooth muscle actin	6
A.u.	Arbitrary units	36
BSA	Bovine serum albumin	24
CL	*Corpus luteum*	4
CTGF	Connective tissue growth factor	6
DAB	3,3′-Diaminobenzidine	24
DTT	Dithiothreitol	28
DNA	Deoxyribonucleic acid	10
ECM	Extracellular matrix	5
EDTA	Ethylenediaminetetraacetic acid	27
EMT	Epithelial-to-mesenchymal transition	6
FELASA	Federation of European Laboratory Animal Science Associations	21
H&E	Haematoxylin and eosin	23
H_2O_2	Hydrogen peroxide	24
HRP	Horseradish peroxidase	24
IHC	Immunohistochemistry	24
IGG	Immunoglobulin G	24
IL-1	Interleukin-1	8
IL-6	Interleukin-6	8
IL-10	Interleukin-10	9
KH_2PO_4	Potassium dihydrogen phosphate	23
M	Molar	23
MMP	Matrix metalloproteinase	5
MNGCs	Multi-nucleated giant cells	10
MW	Molecular Weight	37
OS	Oxidative stress	6
O_2^-	Superoxide anion	47
O_2	Oxygen	47
Na_2HPO_4	Disodium phosphate	23
PBS	Phosphate buffered saline	23
PFA	Paraformaldehyde	21

Abbreviation	Definition	Page
PPAR-γ	Peroxisome proliferator-activated receptor gamma	6
Rep. Aged	Reproductively aged	21
ROS	Reactive oxygen species	10
Sa-β-gal	Senescence-associated β-galactosidase	10
SASP	Senescence-associated secretory phenotype	11
SEM	Standard error of the mean	30
SBB	Sudan Black B	23
SDS	Sodium dodecyl-sulfate	28
TBS	Tris-Buffered Saline	29
TGF- β1	Transforming growth factor beta 1	6
TIMP	Tissue inhibitors of matrix metalloproteinase	6
TNF-α	Tumour necrosis factor α	8
Tx	Triton-X	27
VEGF	Vascular endothelial growth factor	6

Abstract

During ovarian ageing, a population of macrophages with senescent-like markers was identified and its accumulation is negatively correlated with the follicle pool and systemic health consequences. Given the growing evidence that cellular senescence is a contributor to oncogenesis, in a senescence-associated secretory phenotype-dependent manner, we aimed to unveil possible links between the observed unique population of macrophages and the presence of ovarian surface epithelium lesions.

Ovaries from young and reproductively aged animals were used: 3- and 9-months old mice; 5- and 24-months old rats. Sudan black B and haematoxylin and eosin staining of sections were used to identify lipofuscin and assess morphological changes, respectively. Immunohistochemistry and western blotting were carried out to analyse IgG accumulation and extracellular matrix remodelling. Additionally, the effect of apocynin (5 mM in the drinking water for 7 weeks) on IgG accumulation and extracellular matrix remodelling was also tested. In the medulla of ovaries of mice and rats, there was a significant age-related increase in macrophages. In addition, sections exhibited age-related enhancement in IgG labelling. These changes were accompanied by an increase in atypical epithelial cells and alterations in the expression pattern of α-smooth muscle actin, namely the appearance of extra western blotting bands with higher molecular weights. Reproductively aged mice treated with apocynin had ovarian IgG labelling similar to juveniles.

During reproductive ageing accumulation of macrophages with a senescent-like phenotype is accompanied by epithelial cell structural changes, which may reflect the onset of pre-neoplastic lesions. The enhanced IgG labelling is likely to be part of the mechanism for macrophage recruitment and activation. In this context, the use of an antioxidant drug may contribute to delay cell changes and ovarian ageing. Additional work is needed to further understand the relationship between senescence and epithelial lesions.

Keywords: Ovarian ageing; macrophage senescence; IgG accumulation; abnormal epithelium; apocynin

Resumo

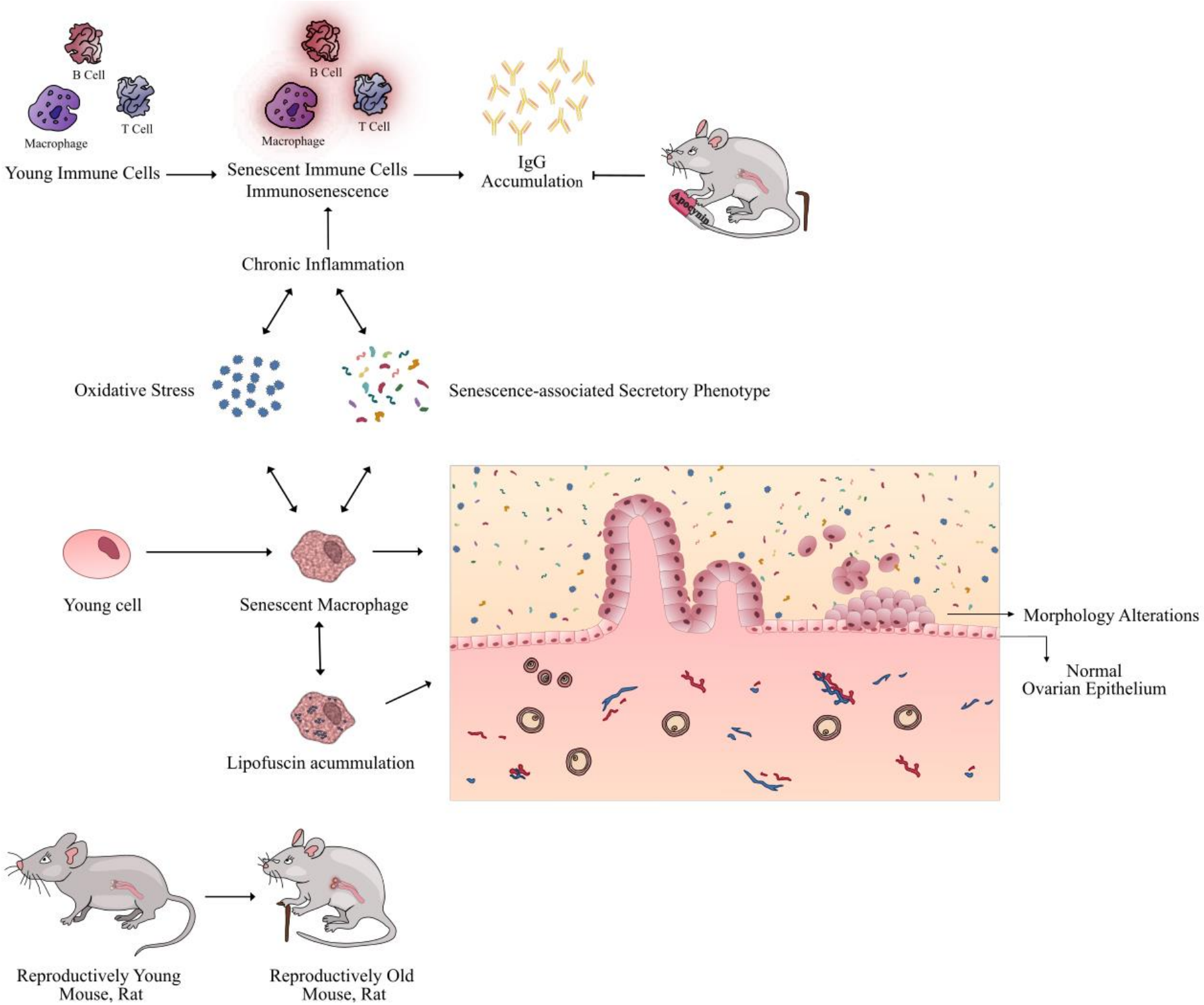
O envelhecimento dos ovários é pautado pela presença de uma população de macrófagos com marcadores semelhantes aos de senescência e a sua acumulação está negativamente correlacionada com o número de folículos e com consequências sistémicas para a saúde. Dada a evidência crescente de que a senescência celular contribui para a oncogénese, de uma forma dependente do fenótipo secretor associado à senescência, o nosso objetivo consistiu em desvendar possíveis ligações entre uma população singular de macrófagos observada e a presença de lesões no epitélio da superfície do ovário.

Foram utilizados ovários de animais jovens e reprodutivamente envelhecidos: ratinhos de 3 e 9 meses de idade; ratazanas de 5 e 24 meses de idade. As colorações com negro de sudão B e hematoxilina-eosina foram utilizadas para identificar depósitos de lipofuscina e avaliar as alterações morfológicas, respetivamente. Imunohistoquímica e *western blotting* foram efetuados para analisar a acumulação de IgG e a remodelação da matriz extracelular. Além disso, foi também testado o efeito da apocinina (5 mM na água de consumo, durante 7 semanas) na acumulação de IgG e na remodelação da matriz extracelular. Na medula dos ovários de ratinhos e ratazanas, verificou-se um aumento significativo de macrófagos associado à idade. Além disso, os cortes histológicos apresentaram um aumento da acumulação de IgG relacionado com a idade. Estas alterações foram acompanhadas por um aumento de células epiteliais atípicas e por alterações no padrão de expressão da α-actina, nomeadamente com o aparecimento de bandas extra no *western blotting* com pesos moleculares mais elevados. Os ratinhos reprodutivamente envelhecidos tratados com apocinina apresentaram uma marcação de IgG nos ovários semelhante à dos jovens.

Durante o envelhecimento reprodutivo, a acumulação de macrófagos com um fenótipo senescente é acompanhada por alterações estruturais das células epiteliais, que podem refletir o início de lesões no epitélio do ovário. É provável que o aumento da acumulação de IgG reflita um mecanismo de recrutamento e ativação de macrófagos. Neste contexto, a utilização de um fármaco antioxidante pode contribuir para retardar as alterações celulares e o envelhecimento dos ovários. São necessários trabalhos adicionais para compreender com mais profundidade a relação entre a senescência e o desenvolvimento ou a progressão de neoplasias.

Palavras-chave: Envelhecimento dos ovários; macrófagos; acumulação de IgG; epitélio anormal; apocinina

Graphical Abstract


B Cell
T Cell
Macrophage
Young Immune Cells
B Cell
T Cell
Macrophage
Senescent Immune Cells
Immunosenescence
IgG
Accumulation
Apoptosis
Chronic Inflammation
Oxidative Stress
Senescence-associated Secretory Phenotype
Young cell
Senescent Macrophage
Lipofuscin acummulation
Morphology Alterations
Normal
Ovarian Epithelium
Reproductively Young
Mouse, Rat
Reproductively Old
Mouse, Rat

Chapter I:
State of Art

I.1 The Ovary

I.1.1 Histomorphology

The ovaries constitute part of the female reproductive system. Their primary function is to mature oocytes, female gametes, and secrete steroidal sex hormones that act as regulators of the reproductive system function and, additionally, affect other systemic organs [1]. Ovaries are shaped as 3 cm long and 1.5 cm wide almonds, coated with a monolayer of squamous-to-cuboidal epithelium, the ovarian surface epithelium. Several adhesion molecules, such as desmosomes, tight junctions, cadherins, and integrins, maintain epithelial integrity and intercellular contact [1]. The innermost part of the ovaries, the medulla, comprises loose connective tissue and blood vessels (**figure 1**) [1]. The cortex makes up most of the ovarian area and is characterized by a stroma of connective tissue and numerous ovarian follicles in many stages of development: primordial, primary, secondary, secondary antral, and Graafian. The stratified squamous epithelium that surrounds follicles is named granulosa, an important source of steroids, such as oestrogen [1]. With the development of primary follicles, granulosa cells secrete follicular fluid, which accumulates and causes small spaces to arise between granulosa cell layers. As the spaces enlarge and cells are rearranged, a large cavity originates, the "antrum", giving rise to the secondary antral follicles, that will develop into the pre-ovulatory follicle – Graafian (**figure 1**).

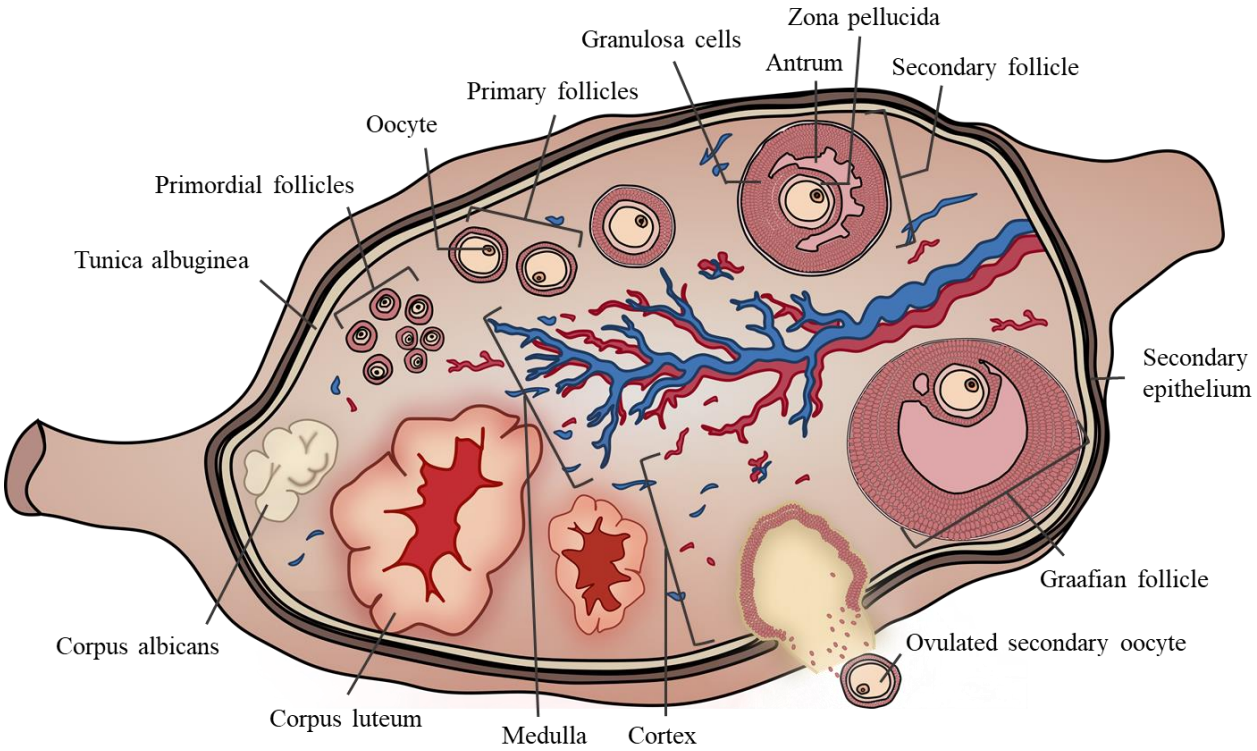


Figure 1: **Ovarian histology and different stages of follicle maturation.** Diagram of a sectioned ovary, picturing different stages of follicle maturation, ovulation and luteal phase.

I.1.2 Ovarian Cycle

Ovulation is an essential biological process in which a mature oocyte is released from the follicle into the oviduct, and it is essentially stimulated by the endocrine system [1,2]. At birth, women present a non-renewable ovarian reserve of approximately 1–2 million immature oocytes. At the beginning of puberty, this number has declined abruptly, to around 400.000 oocytes, continuing to fall throughout the reproductive lifespan [3,4]. When menopause is reached, at approximately 50 years of age, follicle reserve has dropped below a thousand follicles; this number is insufficient to sustain ovarian cycle and consequently, the remaining follicles tend to degenerate [3,4].

The ovarian cycle is divided into follicular phase, ovulation, and luteal phase (**figure 2**). The regulation of such stages is dependent on hormonal interactions secreted by the hypothalamus, the anterior pituitary, and the ovary [2,5-7]. In the follicular phase, a cohort of primordial (inactive) ovarian follicles is recruited and starts developing [3,4,8,9]. Follicles develop at different rates and, in humans, usually only one antral follicle, the dominant follicle, will reach the late follicular phase, the Graffian follicle. The remaining follicles undergo atresia. After ovulation, the granulosa cells undergo luteinization and form the *corpus luteum* (*CL*), a transient endocrine structure that secretes oestrogens and progesterone [10,11]. If pregnancy does not occur, *CL* degenerates, a scar of dense connective tissue–*corpus albicans*–is formed, and the menstrual cycle is renewed [3,4,8,9].

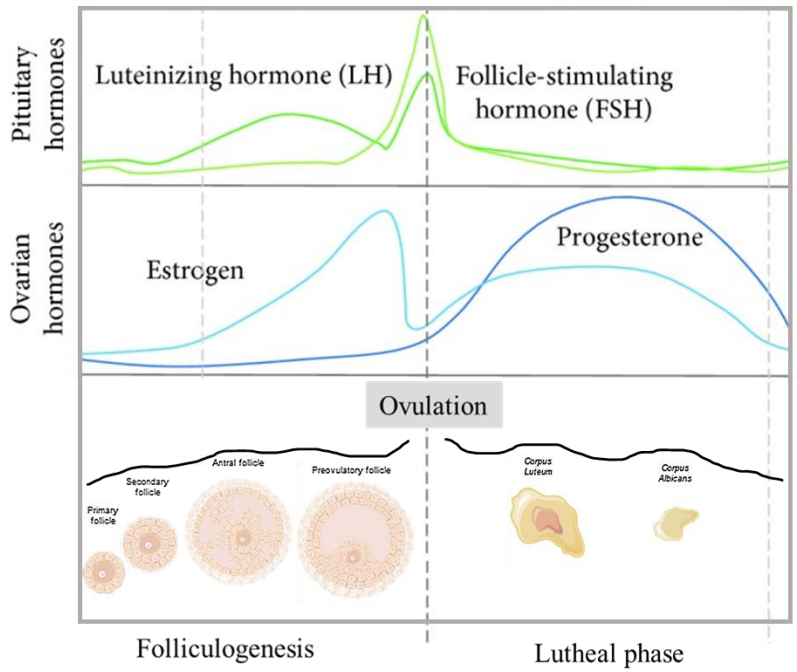


Figure 2: Diagrammatic representation of the different phases of the ovarian cycle and main regulatory hormones, ovarian and pituitary. Image adapted from Mendes, S. *et al*, "New Insights into the Process of Placentation and the Role of Oxidative Uterine Microenvironment" and Timoteo-Ferreira, F *et al*, "Redox imbalance in age-related ovarian dysfunction and perspectives for its prevention".

I.2 Tissue Remodelling and Wound Healing in Ovulation

I.2.1 Wound Healing

Women undergo circa 400-450 ovulations throughout their reproductive lifespan, averaging 40 fertile years with, approximately, 12 ovulations per year [3,12]. Thus, ovulation is a great example of one of the most active physiological wound repair processes in the organism.

During follicular rupture, proteases are released from follicular cells to degrade the extracellular matrix (ECM), allowing the creation of an opening for oocyte expelling. Ovary-resident macrophages produce, as well, matrix metalloproteinases (MMPs) that participate in ECM breakdown [13]. This process damages the stroma and the ovarian surface epithelium overlying the ovulatory follicle [2,5-7]. In its healthy performance, the ovary repairs itself hastily; in mice, it can be repaired in as little as 12 hours [2,14].

Wound healing in the ovary follows three classic stages common to the majority of tissues: inflammation, proliferation, and remodelling [15,16]. After ovarian surface epithelium rupture, platelets are activated and release factors that attract activated immune cells into the wound, namely macrophages to phagocytose debris from atretic follicles and the released oocyte – inflammatory phase [15]. Next, the proliferative phase initiates, in which cells (endothelial cells, fibroblasts, among others) proliferate and migrate in order to repair the tissue [15]. Meanwhile, macrophages promote angiogenesis and release anti-inflammatory cytokines, resolving the inflammation [17]. This generates a preliminary, vascularized ECM that matures during the remodelling phase, after stimulation by growth factors, resulting in a collagen-rich scar (**figure 3**).

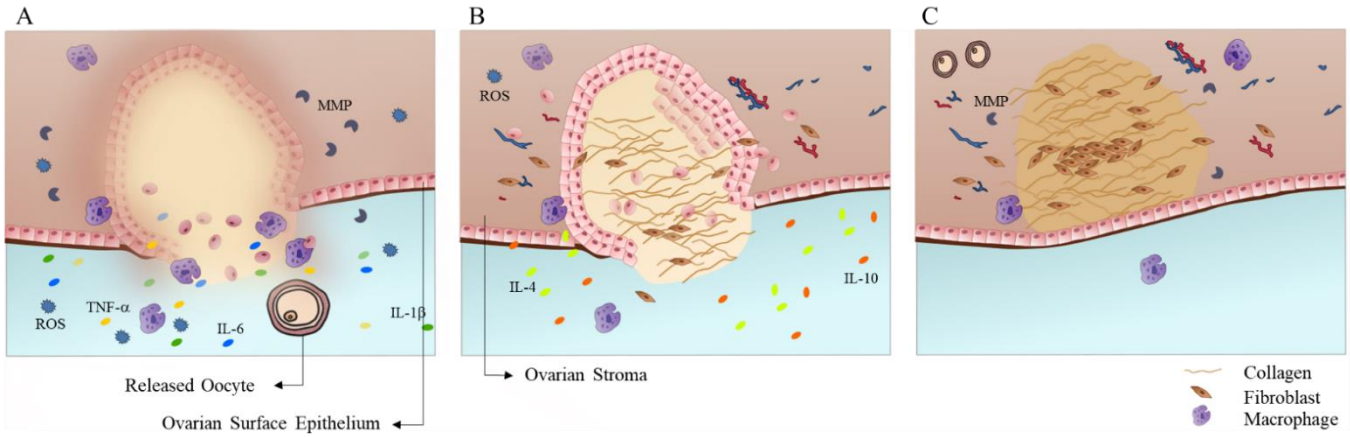


Figure 3: **Post-ovulatory wound healing.** Acute wounds progress through the phases of inflammation, proliferation, and remodelling, depicted, respectively, in A-C images. (A) Pro-inflammatory macrophages are recruited to phagocytise dead cells and debris, and secrete inflammatory cytokines (tumour necrosis factor-α, IL-6 and IL-1β), vascular permeability factors, and proteases that enhance the recruitment of immune cells into the wound. (B) Cells from the vicinity of the wound and epithelium migrate into the wound, and new blood vessels now populate the area. The dividing fibroblasts deposit collagen and shift the wound microenvironment from the inflammatory to the growth state. Pro-wound healing macrophages are present, secreting factors that aid in

angiogenesis, collagen deposition, and re-epithelialization. (C) Macrophages secrete metalloproteinases to aid cellular migration and maturation of collagen, and engulf excessive extracellular matrix (ECM), to return tissue homeostasis. Unregulated deposition of ECM can lead to fibrosis [12,15,18].

Epithelial-to-mesenchymal transition (EMT) also plays a crucial role in wound repair, by allowing migration of cells into the wound to aid the re-epithelialization process [19]. EMT is a transient, essential process for wound healing and tissue regeneration in adulthood, in which epithelial cells acquire a mesenchymal phenotype, namely increased motility and invasive capability, as well as resistance to hypoxia and oxidative stress (OS); expression of markers of EMT, as α-smooth muscle actin (α-SMA), vimentin, fibronectin and N-cadherin, are also increased [14,19-25]. Cytokines abundant in preovulatory follicular fluid, such as transforming growth factor beta 1 (TGF-β1), produced by granulosa cells and macrophages, are capable of inducing an EMT response [19].

I.2.2 Fibrosis

During ovarian wound healing and repair stages, the mechanism of fibrogenesis is activated, and quiescent fibroblasts are exposed to growth factors and cytokines [including MMPs, tissue inhibitors of matrix metalloproteinases (TIMPs), TGF-β1, connective tissue growth factor (CTGF), peroxisome proliferator-activated receptor gamma (PPAR-γ), vascular endothelial growth factor (VEGF)] produced by macrophages (**figure 4**) [26]. This results in fibroblast activation, further transformation into myofibroblasts, and stimulation of collagen deposition in the wound, with simultaneous secretion of collagenases [27]. Macrophages can also deposit ECM components themselves. Expression of α-SMA is indicative of increased collagen accumulation [28]. Evidence points out that age-associated changes in ovarian ECM occur as oestrogen levels fall, resulting in fibrosis [29,30]. Fibrosis is characterized by excessive deposition of fibroblasts and ECM proteins, namely collagen I and III, due to its deficient degradation, and was previously observed in the ovaries of aged mice [28,30]. Ovarian fibrosis can be triggered by ovarian injury– inflammation, surgery, immune abnormalities –, in which the mutually interacting growth factors and cytokines disrupt the balance between ECM synthesis and degradation (**figure 4**) [26]. A previous study found an association between aged fibrotic ovaries and chronic inflammation [28].

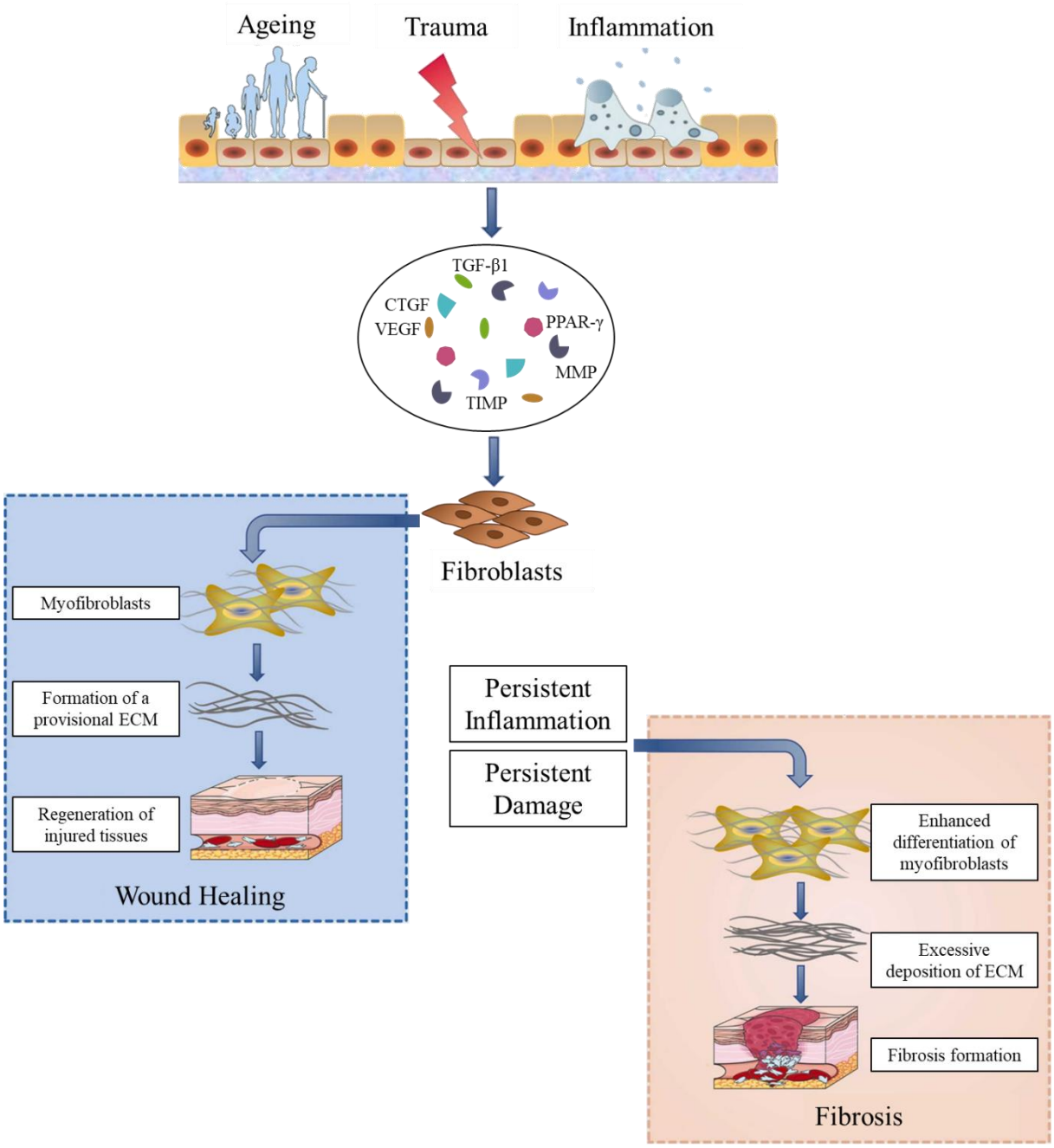


Figure 4: **Process and pathogenesis of organ fibrosis**. Damage caused by various stimuli, such as ageing, trauma or inflammation, lead to the release of cytokines and growth factors to induce fibroblast activation and generation of temporary extracellular matrix (ECM) for the regeneration of injured tissues. Persistent damage and inflammation cause excessive accumulation of ECM, ultimately leading to tissue fibrosis. Image adapted from Yang *et al*, "Aryl hydrocarbon receptor: From pathogenesis to therapeutic targets in aging-related tissue fibrosis".

I.3 Inflammatory Processes in Ovulation

I.3.1 Innate and Adaptive Immunity and Inflammageing

The immune system is not only responsible for maintaining organism homeostasis but also plays a crucial role in many fertility-related events and in the regulation of the ovarian cycle [31]. Populations of leukocytes, such as macrophages, dendritic cells, and T and B lymphocytes typically comprise the physiological milieu of the female reproductive tract, particularly the ovaries [32-35]. Cytokines produced by ovarian or immune cells modulate ovarian development, by regulating the secretion of steroid hormones, stimulating follicle maturation, ovulation, formation of the *CL* [31,36-39].

The immune system is divided into two main branches: the innate and the adaptive immunity [40]. The innate immunity is the body's first line of defence, including physical barriers (skin), cellular components (macrophages, neutrophils, which recognize general molecular pattern–pathogen-associated molecular patterns and damage-associated molecular patterns–and phagocyte target cells), and soluble factors [complement proteins, pro-inflammatory cytokines, such as, interleukin-1 (IL-1), tumour necrosis factor-α (TNF-α), and interleukin-1 (IL-6), that play crucial roles in inducing inflammation] (**figure 5**) [40]. Overall, the innate response lacks specificity and immunological memory, in contrast to the adaptive immunity, which targets specific antigens through highly specific receptors on B and T lymphocytes [40]. B cells produce antibodies that neutralize pathogens and mark them for destruction by other immune cells, while T cells help activate ($CD4^+$ T cells) or directly kill infected cells ($CD8^+$ T cells) [40].

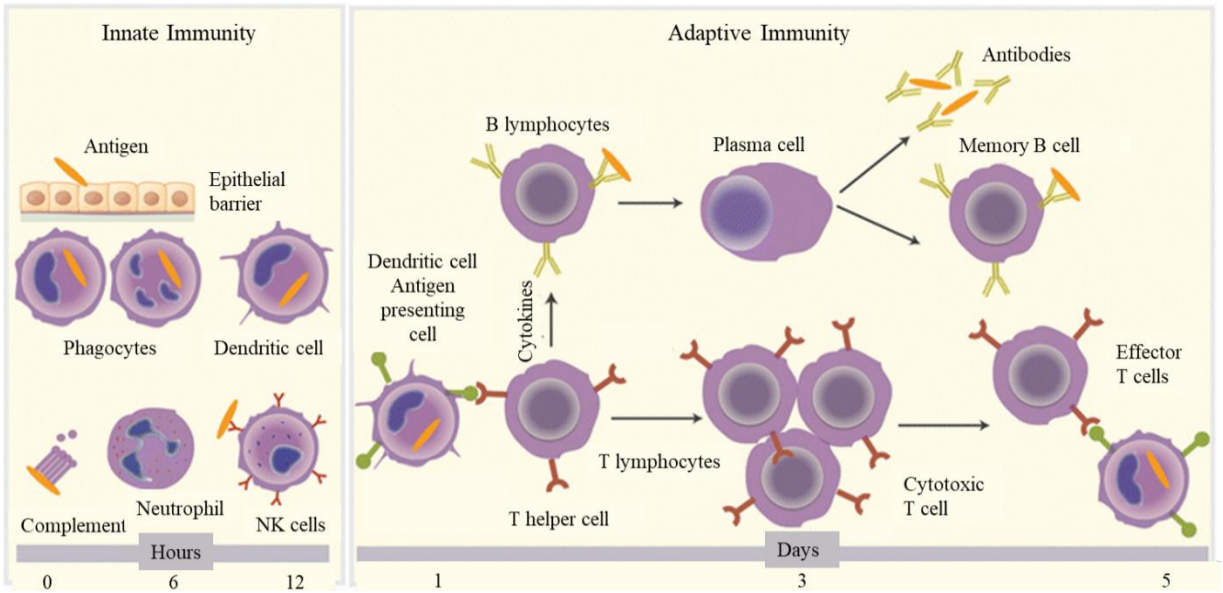


Figure 5: The basic components of the innate and adaptive immune responses. Image from Mehta, K. *et al*, Immunotherapy in genitourinary malignancies.

Whilst immune system pathways are key for the steady functioning of the ovary, their dysregulation leads to a handful of pathologies, such as premature ovarian failure, polycystic ovary syndrome or inhibited steroidogenesis in granulosa cells [6,41-45]. With the advancing of age, there is a systemic deterioration of the adaptive immune system, and an increase in innate immune activity [18]. This is manifested through enhanced levels of natural killer cells and pro-inflammatory cytokines, likely released by macrophages [18].

Balancing pro- and anti-inflammatory responses is essential for successful ageing [46]. Exposure to pathogen-associated molecular patterns and danger-associated molecular patterns disrupts the balance between pro-inflammatory networks, which combat recognised threats, and anti-inflammatory networks, which maintain homeostasis [46]. After a prolonged period of oxidative and inflammatory stress generated by these molecular patterns, the tissue microenvironment switches to a state of chronic inflammation [21,47-50].

This chronic activation of inflammatory responses, induces changes in the surrounding microenvironment, with production of enhanced levels of proinflammatory cytokines (IL-1β, interleukin-α, IL-6, interleukin-8, TNF-α), likely released by macrophages, resulting a low-grade chronic inflammatory response [18]. Its persistence, characteristic of the elderly, can become pathogenic, generating an inflammatory state entitled "Inflammageing" and is being explored in the context of age-dependent diseases, namely Type II diabetes, atherosclerosis, and cancer [18,33,46,51-53].

I.3.2 Macrophage-induced Inflammatory and Oxidative Microenvironment

It has been proposed that macrophages exacerbate age-associated inflammation within the ovary [54]. Macrophages are mononuclear, phagocytic cells that are central to innate immunity [18]. They are highly abundant in the mammalian ovary and display strong plasticity in their phenotypes and functions when exposed to various tissue microenvironments [29]. In the ovaries, they perform several secretory and phagocytic roles in processes such as folliculogenesis, ovulation, and tissue organization setting a pro- or anti-inflammatory environment according to each stage of wound healing: they are present in the thecal layer of growing follicles, contributing to follicular growth via the release of cytokines and growth factors; they promote granulosa cell proliferation, vascular growth, follicle development, and steroid hormone production; they also promote ovulation through cytokine secretion and ECM breakdown and facilitate luteolysis through TNF-α [13,18,27,29].

Inflammatory cytokines/chemokines released during inflammageing promote macrophage polarization into two subpopulations based on the expressed surface markers and biological activities: classically activated M1 macrophages and alternatively activated M2 macrophages [29]. M1 macrophages are induced by pro-inflammatory signals (interferon-γ, TNF-α, granulocyte-macrophage colony stimulation factor) and generate chemokines and pro-inflammatory cytokines [TNF-α, IL-1α/β, IL-6, interleukin-12, interleukin-18 and interleukin-23) [29]. In young ovaries, M1 macrophages are involved in primordial follicle activation [29]. M2 macrophages are induced by anti-inflammatory signals [interleukin-4, interleukin-13 and interleukin-10 (IL-10)] and generate anti-inflammatory cytokines (IL-10 and TGF-β), fibroblast

growth factor and platelet-derived growth factor, which facilitate inflammation resolution, tissue repair and fibrosis. In young ovaries, M2 macrophages maintain follicles in a dormant state [29]. These phenotypes also play distinct roles in ovarian ageing: in the early stages of ovarian ageing, the M1 phenotype is increased and promotes pro-inflammatory gene expression. However, in later stages, M2 macrophages are predominant and contribute to ECM deposition, ultimately leading to ovarian fibrosis [29].

In histological sections of reproductively old mice ovaries, a unique population of cells that resemble hyperactivated macrophages, has been identified, designated multinucleated macrophage giant cells (MNGCs) [18,29,30,55,56].

While the role of MNGCs is not yet elucidated, it might indicate a failure of normal physiology, considering observations of similar giant cells in other tissues [18]. MNGCs are specialized phagocytic cells, frequently associated with a broad variety of chronic inflammatory conditions, namely pulmonary granulomas in tuberculosis, parasitic infections and sarcoidosis [57]. MNGC generation is thought to result from macrophage fusion in an attempt to phagocytise large particles, which macrophages are not able to efficiently phagocytose, and remove collagen-dense fibrotic foci and other cell debris deposits, such as lipofuscin [13,18,28,29][58-63]. Although the presence of some M2 macrophage-associated markers (arginase 1, resistin-like molecule alpha) positively correlates with the increased presence of MNGCs in aged ovaries, the relationship between these two cell populations in the ovary is not yet validated [18].

Emerging evidence suggests that MNGCs may acquire senescent-like properties, including increased expression of senescence-associated markers such as: 1) enlarged nucleus and altered cell morphology, 2) enhanced expression of cyclin-dependent kinase inhibitors, p21 and p16 (cell cycle inhibitors), 3) an increased activity of lysosomal senescence-associated β-galactosidase (SA-β-gal), 4) loss of nuclear lamin B1 or 5) lipofuscin accumulation (**figure 6**) [35,62,64-71]. Cellular senescence can be defined as a state of permanent growth arrest in the G1 phase of the cell cycle as a damage response to excessive cellular stress – deoxyribonucleic acid (DNA) damage, excessive reactive oxygen species (ROS), inflammation, organelle dysfunction (mitochondrial dysfunction), telomere shortening, oncogenic activation – aiming to limit the proliferation of damaged cells and impair potential malignant transformation (**figure 6**) [34,48,69-72].

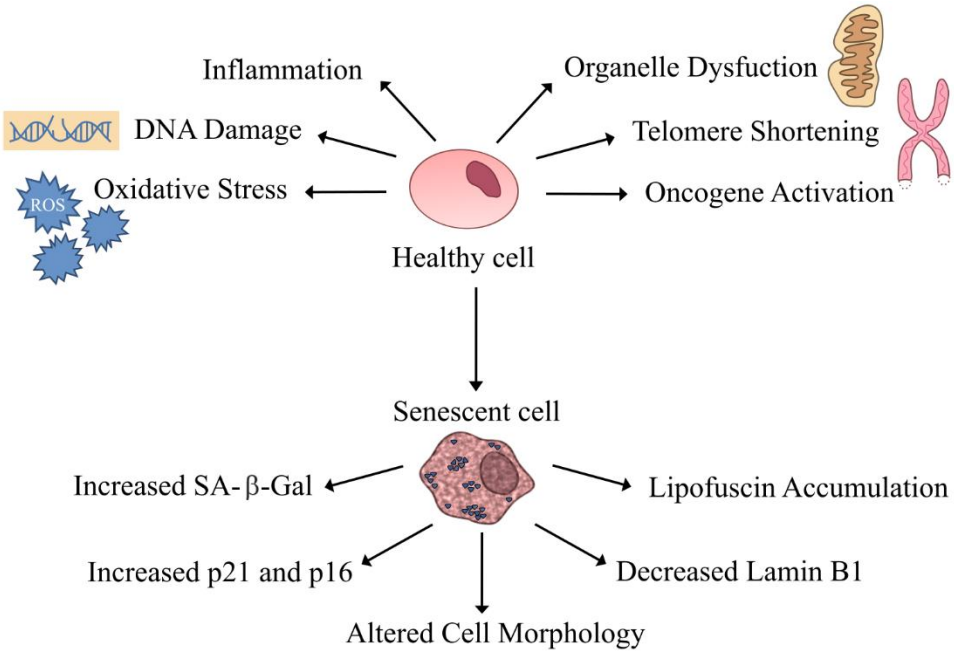


Figure 6: **Potential causal factors and hallmarks of cellular senescence.** Senescence is a damage response to cellular stressors such as DNA damage, mitochondrial dysfunction, oxidative stress, inflammation, or oncogene activation. The damage responses activated lead to enhanced expression of p21 and p16, aberrant cell morphology, loss of lamin B1, and increased SA-β-gal activity [69-71].

It has been reported that MNGCs accumulate in the ovaries of reproductively aged mice, mature sheep and goats and correlate negatively with age-associated follicle pool depletion [30,68,73]. Since senescent and senescent-like cells retain their viability and functionality, their active metabolism enables the secretion of specific factors that comprise MMPs, proteases, chemokines, proinflammatory cytokines (as IL-1α, TNF-α and TGF-β), and growth factors, among others [74], all together they comprise what is called a senescence-associated secretory phenotype (SASP) [30,67,74,75]. SASP is known to stimulate the immune system to clear damaged cells and repair the surrounding tissue after damage, in a wound healing mechanism [21,47-50]. However, SASP promotes a state of exacerbated inflammation [21,49,50]. In the ovaries, MNGCs with a senescent-like phenotype may further exacerbate the proinflammatory microenvironment by secreting SASP components [76].

I.4 Ovarian Ageing and Cancer

Ageing represents the inevitable decline of organs' function over time, accompanied by an increased vulnerability to develop age associated diseases, such as cardiovascular disease, diabetes, neurodegenerative diseases (Alzheimer and Parkinson diseases), hyperplasia and cancer development (circa 60% of individuals diagnosed with different types of cancers are, at least, 65 years), among other co-morbidities [77-81]. Ovaries are no exception to this process: they undergo ageing much earlier in life in comparison to most organs, starting approximately halfway through a woman's lifespan, which entails health and social problems [82,83].

Cells continuously face damaging agents and stressors throughout life, undergoing cellular senescence. Considering that senescent cells survive long periods and are more resistant to apoptotic signals than normal cells, there is an accumulation of senescence burden in tissues throughout the life of an individual [21]. It has been reported that a rare cancer of the ovaries, Sertoli-Leydig cell tumour, can exhibit lipofuscin in Leydig cells [84,85]. Moreover, SASP factors orchestrate a propitious inflammatory and oxidative microenvironment propitious for uncontrolled proliferation of damage-harbouring cells, as well as cellular hyperactivity, resistance to apoptosis, and migration capacity, culminating, ultimately, in the onset of neoplasms or even tumour progression [81,86-92].

In 1971, Fathalla *et al*. proposed the "incessant ovulation hypothesis", which suggests that genomic disturbances arise in the ovarian surface epithelium during the repeated cycles of ovulation and derived wound healing repair. It is proposed that intense proliferation of epithelial cells during *CL* regression and ECM and ovarian surface epithelium remodelling may propagate mutations or promote carcinogenesis [14,93]. Epidemiological data indicates that factors known to suppress ovulation, such as the use of oral contraceptive pills and pregnancy, are associated with a decreased incidence in ovarian cancer. Regions where the use of oral contraceptives started earlier and is more widespread, such as Northern and Western Europe, present more favourable trends in ovarian cancer, in contrast to Central and Eastern Europe, where the use of oral contraceptives started later [94]. Studies have shown a direct correlation between the number of ovulatory cycles and the risk of epithelial ovarian carcinogenesis [27,93,95,96].

Increased number of inclusion cysts, resulting from invaginations of the ovarian surface epithelium, are also associated with ovulation rates [97]. Metaplasia of ovarian surface epithelial cells within these cortical inclusion cysts has been suggested as a putative pathological change leading to ovarian cancer, and occasional cases of ovarian intraepithelial neoplasia have been identified in inclusion cysts or on the ovarian surface epithelia [98-100]. Furthermore, after ovulation, EMT is activated in wound repair, allowing migration of cells into the wound to aid the re-epithelialization process [19]. Upon EMT, epithelial cells acquire mesenchymal traits, granting them enhanced migratory and invasive capability, and a less differentiated phenotype, as well as resistance to hypoxia and OS [14,19-25]. Dysregulation of this tight mechanism can be crucial for metastatic evolution and tumour development [21,89,101]. Yet in the sphere of tissue repair, age-related induction of fibrosis in the ECM has been linked to tissue dysfunction in the ovary and may favour neoplasm development [2,28,35,102-104]. It is known that progression of tumour cells is followed by alterations in cell composition and ECM [105,106].

Although cancer and ageing seem distinct processes, both can be seen as distinct outcomes stemming from a common origin [79]. It is believed that SASP and senescent response have pleiotropic effects. On the one hand, irreversible replicative arrest protects against tumourigenesis by preventing the proliferation of cells at risk for malignant transformation [107], but on the other hand, increase of senescent cell burden in later stages of life, chronic exposure to SASP factors, particularly inflammatory events, and to lipofuscin-induced OS, may affect tissue homeostasis and induce neoplasms [86-88].

Regardless of the growing evidence linking repeated ovulatory cycles with ovarian cancer onset and progression, the underlying mechanisms of its oncogenesis remain, yet, unclear, akin to the intricate crosslinks between cellular senescence, ovulation and alteration in ovarian surface epithelium.

Chapter II:
Hypothesis & Aim

Providing the accumulation of senescent cells in mammalian tissues during ageing, and the growing evidence linking cellular senescence to oncogenesis, we aimed to investigate the relationship between the observed accumulation of macrophages with a senescent-like phenotype, thought to be ovulation-related, and the presence of ovarian surface epithelium abnormalities (that are known to give rise to neoplastic lesions, such as ovarian epithelial tumours) [108].

To substantiate the postulated hypotheses, three primary goals were established:

→ To trace a more evident cause-effect correlation between presence of MNGCs and recruitment of inflammatory immunoglobulins;
→ To evaluate the age-related presence of abnormalities in ovarian surface epithelium and extracellular matrix remodelling;
→ To analyse the influence of parity in the context of ovarian ageing.

Chapter III:
Materials & Methods

III.1 Animal Handling and Ovarian Tissue Collection

We conducted this study with ovaries collected from female mice and rats. Female mice (C57BL/6J strain) obtained from Harlan and female rats (Wistar strain) from Sprague Dawley were housed at Instituto de Investigação e Inovação em Saúde (i3S) and Faculty of Medicine of Porto University facilities, respectively. All the experiments were performed according to the Portuguese law on animal welfare and according to the guidelines issued by the Federation of European Laboratory Animal Science Associations (FELASA).

Animals were kept under controlled conditions of light and temperature (12-hour light/dark cycle and room temperature of 22 °C) and had free access to tap water and standard chow. A subgroup of reproductively aged mice was treated with apocynin: the administration of the antioxidant was done at a concentration of 5 mM, in drinking water 7 weeks prior to sacrifice. Water bottles were protected from light and changed twice a week. Moreover, the handled rats were nulliparous, and part of the mice group was composed of nulliparous specimens, while the other consisted on multiparous animals.

Reaching the selected ages, the animals were anesthetized with isoflurane and ovaries were excised. One of the ovaries was immediately frozen in liquid nitrogen and kept at -80 °C for molecular studies, while the other was fixed overnight, in 4 % paraformaldehyde (PFA), for structural studies.

The experimental animal set-up used in this study is depicted in **figure 7.**

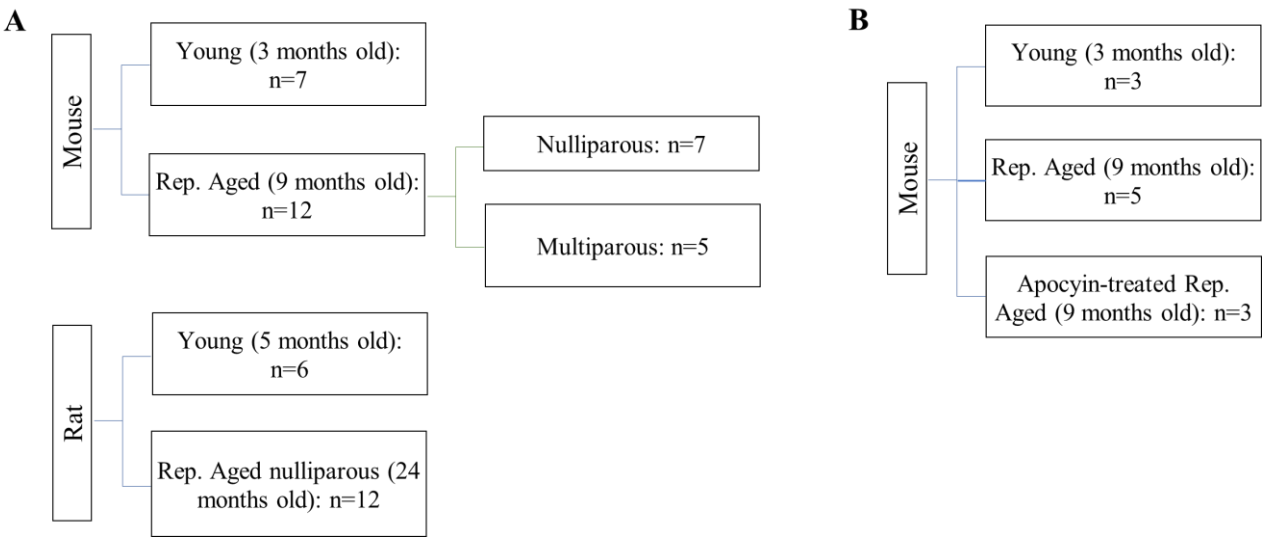


Figure 7: Simplified diagram of the experimental animal set-up used in this study, describing the number and age of the studies animals. "Rep. Aged" is the abbreviation for "Reproductively Aged". **(A)** Depicts the set-up used in staining and immunohistochemistry techniques. **(B)** Depicts the set-up for western blotting, in which all reproductive aged mice were nulliparous.

III.2 Tissue Processing, Fixation and Sectioning

Sample fixation prevents the deterioration of tissue, cells and antigens, as well as its autolysis and necrosis, hence the urge in quick fixation of the tissue right after its harvesting. Paraffin embedding offers support during sectioning, and it is the step that follows fixation.

A solution of 4 % PFA was used as fixative for 24 hours, followed by tissue dehydration applying increasing concentrations of ethanol, withdrawing excess fixative and preparing the tissues for paraffin embedding. Tissues were dehydrated as follows: 70 % alcohol (E/0650DF/C17, Fisher Chemical) overnight, 70 % alcohol for 30 minutes, 90 % alcohol for 1 hour (renovation of the ethanol after 30 minutes), proceeding to immersion in absolute alcohol, for 1 hour (renovation of the ethanol after 30 minutes). Then, tissues were diaphanized in xylol at 97 % (905-562-9, Valente e Ribeiro Lda.) for 40 minutes, embedded in pre-heated paraffin (at 60 ºC) for 1 hour and, lastly, placed in new paraffin for another hour. Paraffin blocks were microssectioned using a microtome (RM2145, Leica Biosystems®) and sequential sections of of 5 µm of width obtained. Sections were placed in coated glass slides and dried overnight at 36 ºC.

III.2.1 Slide Coating

Slide coating consists in a histological adhesive that allows an eased anchorage of paraffin sections onto glass slides. Poly-L-lysine (P8920, Sigma), an electrostatic adhesive, is one of the most common coatings, and was used for slide coating, promoting nonspecific adhesion of tissue sections to the glass. The slides were rinsed with a cloth embedded in absolute alcohol, finally, and immersed in previously filtered poly-L-lysine for 5 minutes. The excess of coating was removed from the slides, carefully hitting them in a plane surface, and then, they were left to dry for 48 hours at 37 ºC.

III.3 Staining Techniques

When it comes to histologic procedures, whether it is histochemistry or techniques that involve sections kept in paraffin, the first step to take into account is paraffin removal from the tissue sections.

Paraffin dissolution was done by placing the slides in xylene, first for 20 minutes and then with a renewed xylene 10 minutes. Afterwards, the sections were hydrated, going through decrescent concentrations of alcohol to remove the xylene (absolute, 90 % and 70 %, for 5 minutes each). From this point on, the remaining protocol may differ depending on the procedure to be performed for the selected staining.

III.3.1 Haematoxylin and Eosin

A greater part of cell and tissue components have no visible colour. Haematoxylin and Eosin (H&E) is the preferred stain technique used for observing a broad range of tissue and cellular architecture, namely nuclear, cytoplasmic, and ECM features, providing a comprehensive picture of tissues microanatomy.

As implied by its name, this technique comprises two staining components: haematoxylin and eosin. The first has no staining properties itself until it has been oxidized to haematein and combined with a mordant, which is typically a metal cation, and allows visualization of the nuclear features, staining heterochromatin and nucleoli purple/blue. This occurs due to attraction of charges: the mordant (positively charged), will bind to negatively charged components, such as nucleic acids. On the other hand, eosin is anionic, binding to positively charged components and dyeing amino groups on proteins in the cytoplasm and red blood cells in shades of pink [109].

After paraffin removal from tissue sections, and hydration, tissues were rinsed in water, and kept in running water for approximately 20 minutes. Afterwards, Modified Harris Haematoxylin (72704, Richard Allan Scientific, Thermofisher) was applied to the sections for 45 seconds, to avoid overstain, colouring the nuclei and some other elements purple/blue. The slides were rinsed, to remove excess dye, and checked to see if the nuclei were properly stained. Next, the sections were incubated with alcoholic solution of eosin (Eosin Y, 71211, Richard-Allan Scientific, Thermo Scientific), in a proportion of 1:5 in 70 % alcohol, for 30 seconds to avoid pink overstaining. The slides were briefly passed through increasing concentrations of ethanol (70 %, 90 %, 100 %), for dehydration, and then, immerged in xylene, for 10 minutes plus 5 minutes in another rack. Mounting medium (Entellan®, 1.07961.0100, Sigma-Aldrich) was applied to the tissue slides and, after drying, preparations were ready to be visualized under the light microscope.

III.3.2 Sudan Black B

Sudan Black B (SBB) is a lipophilic dye considered to be sensitive and specific for lipid identification. It is used to stain lipid-containing structures, namely phospholipids and intracellular lipids: lipoproteins, neutral lipids and lipofuscins, which contain insoluble lipids derived of lysosomal digestion [110,111]. In paraffin-embedded tissues, organic solvents used in dewaxing and hydration lead to a great loss of lipids, but lipofuscin's insoluble nature allows it to remain intact, and therefore, it may be visualized with this technique [110,112].

Ovarian sections were dewaxed and hydrated as previously mentioned, until reaching 70 % ethanol, and then stained with 1 % SBB (Sigma-Aldrich, 199664) for 1 hour. Afterward, tissues were rinsed in 70 %, ethanol to differentiate the overstained background from the lipofuscin staining, rinsed in phosphate-buffered saline (PBS) –0.137 M sodium chloride, 0.0027 M potassium chloride, 0.01 M disodium phosphate (Na_2HPO_4), 0.0018 M potassium dihydrogen phosphate (KH_2PO_4), and then mounted in Aquatex® aqueous mounting medium.

Lipofuscin presence was detected using a light microscope (Zeiss Axioskop 40) equipped with a digital camera (Zeiss AxioCam 208 Color).

III.4 Immunohistochemistry

Immunohistochemistry (IHC) is a technique that combines histological, immunological and biochemical techniques. Antigens, such as cellular or tissue components, can be identified through reaction with specific antibodies, which allows for their visualization by optical microscopy [113].

The IHC conducted in the present study deviated slightly from the standard protocol, since our aim was to detect immunoglobulins G (IgGs) in ovarian tissues (**figure 8**). **Table 1** summarises the antibodies used to conduct the experiments, anti-mouse (in mouse tissues) or anti-rat (in rat tissues).

Ovarian tissue sections were dewaxed and hydrated as previously mentioned. Afterwards, heat-induced antigen retrieval was performed. Citrate buffer (2.3 g sodium citrate/L of water (MB01501, Nzytech), pH= 5.75) was heated until boiling and tissue sections were submersed in it right away and kept at 65 ºC for 30 minutes. After successive rinses with PBS (three times 10 minutes), we used H_2O_2, a common peroxidase blocking agent, to quench endogenous peroxidase activity. It allows us to avoid non-specific staining, since ovarian tissues are not devoid of endogenous enzymes, namely peroxidase activity. The blocking solution was done by adding 30 % (v/v) hydrogen peroxide (H_2O_2) to methanol, in a dilution 1:10, and the sections were incubated in this solution for 30 minutes, at room temperature. Then, they were rinsed three times with PBS. To reduce background staining, slides were treated with 5 % bovine serum albumin (BSA) in PBS for 1 hour, at room temperature. Afterward, the slides were incubated with the antibody with horseradish peroxidase (HRP) enzyme (see **table 1**), overnight at 4ºC in a humid chamber. The antibody was diluted in the blocking solution to ensure optimal conditions for specific binding. The following day, tissues were washed three times in PBS, for 10 minutes each. For the detection step, a chromogen system was used, in which the HRP-conjugated antibody catalysed the oxidation of 3,3'-diaminobenzidine (DAB) by H_2O_2. A 0.06% DAB solution in PBS was mixed with H_2O_2 at a 1:1000 ratio. The tissues were incubated with this solution at room temperature until it was observed a specific brown staining. This staining corresponds to the formation of an extremely stable precipitate at the antigen location, allowing for long-term observation using light microscopy. Finally, the tissues were rinsed with PBS, for 5 minutes, followed by distilled water, counterstained with haematoxylin, rinsed again in water, dehydrated through a series of increasing ethanol concentrations (70 %, 90 % and absolute), cleared in xylene, and mounted in Entelllan®.

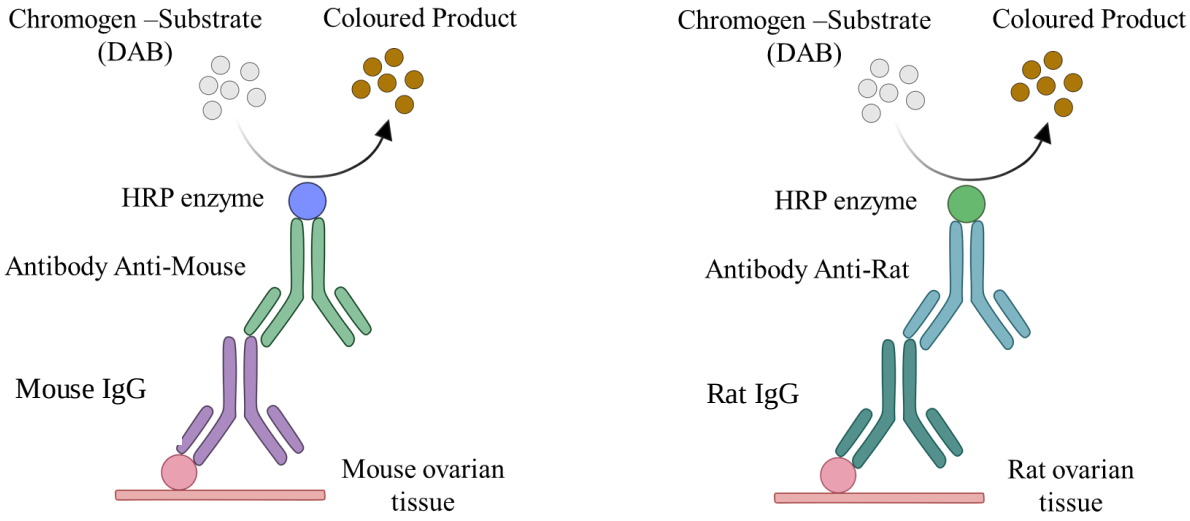


Figure 8: **Schematic image of IHC procedure**. Antibodies raised in the same species as the target tissue were chosen, allowing cross-reactivity and detection of IgG in the tissue.

Table 1: List of antibodies used for IHC technique.

Primary Antibodies	Dilution	Conjugation	Provider
AffiniPure Donkey Anti-Mouse	1:200	Peroxidase-conjugated	715-035-150 Jackson ImmunoResearch
AffiniPure Goat Anti-Rat	1:200	Peroxidase-conjugated	AB_2338128 Jackson ImmunoResearch

III.5 Stained Sections Analysis and Quantification

Lipofuscin was identified using SBB staining. Images of complete mid-ovarian sections were captured. The total mid-section and stained areas were quantified using the Image J software, version 2.0, by identification of the colour threshold cut point, according to **figure 9A**, with the blind intervention of two operators. A minimum of five animals per group was analysed, and two mid-ovarian sections of each ovary were evaluated. The quantification of each stained area was conducted by calculating the ratio of the obtained stained area over the overall area of the respective ovary mid-section.

The brownish IgG staining was also quantified using Image J software, through identification of the threshold cut point (**figure 9B**), in a similar manner to which of **figure 9A**, but following a different colour recognition pattern. A minimum of five animals per group was analysed, and two ovarian mid-sections of each ovary were evaluated. The quantification of the IgG-stained area followed a similar procedure to that of SBB, by calculation of the stained area ratios.

Lastly, evaluation of abnormal epithelia was conducted and, once again, two ovarian mid-sections of a minimum of five animals per group was analysed. The total perimeter of the mid-sections was calculated using Image J, by manual demarcation of the section's limits, as can be observed in **figure 9C**. The measurement of the abnormal perimeter was done manually via a qualitative appreciation: abnormalities in the epithelium were considered when it exhibited:

- a sequence of cells with an elongated morphology that contrast with the squamous-to-cuboid cells of the normal epithelium;
- papillary growths;
- loci where epithelial cells were arranged in multilayers;
- epithelial shedding, or an evident range of cells that seemed to be detaching from the ovarian surface.

The length of the abnormal perimeter was measured in the same manner as the total perimeter, and a ratio of abnormal perimeter over total perimeter was calculated. The average values for each age group and each animal were determined (**figure 9A**).

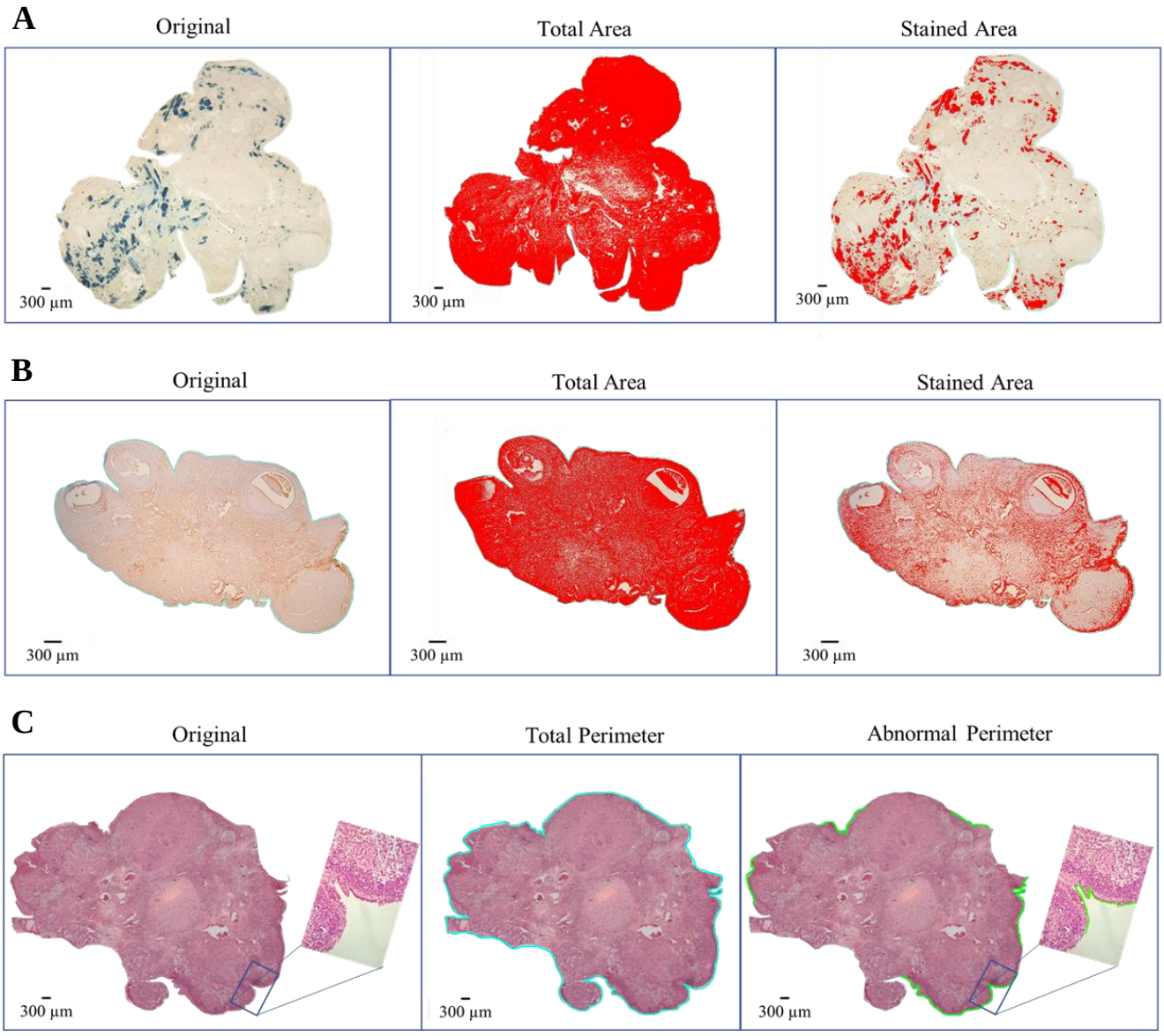


Figure 9: **Representative images of ovarian mid-sections depicting the measurement methods in Image J software. (A)** Threshold cut point determination used for SBB staining relative quantification. **(B)** Threshold cut point determination used for IgG staining relative quantification. **(C)** Perimeter considered abnormal used for relative quantification. The ovaries presented were collected from two rep. aged rats (A and C), and a rep. aged mouse (B).

III.6 Tissue Lysis

The extraction of proteins from tissues requires lysis and disruption of cell membranes, using mechanical homogenization and/or sonication. To start with, ovarian tissues were submersed in 100 µL of ice-cold lysis buffer solution [50 mM Tris base (MB01601, Nzytech), 10 mM NaCl (MB15901, Nzytech), 5 mM ethylenediaminetetraacetic acid (EDTA, EDS-500 g, Sigma Aldrich) and 0.25% Triton X-100 (Tx-100, T9284, Sigma-Aldrich)], containing protease (P8340-5ML, Sigma Life-Science) and phosphatase (Kapa Biosystems) inhibitors, in a proportion of 1:200 and 1:500, respectively. Tubes with the tissue, homogenization buffer and

zirconium oxide (1.4 mm) beads were placed in a MagNA Lyser device and underwent three cycles of mechanical homogenization. Cycles were performed as indicated: 15 seconds at 6500 rpm speed, intercalated with observation and cooling of the samples in ice. The samples were left in ice for 20 minutes, and, afterwards, sonicated at 4 ºC in Biorupter® UCD-200. Two cycles of 10 minutes were performed. Then, sonicated samples were centrifuged at 16 000 g for 10 minutes, at 4 ºC, and the supernatant was stored at -20 ºC for future experiments.

III.7 Protein Quantification

In order to proceed to Western Blotting and to apply equal amounts of protein to the electrophoresis gel, it is imperative to know protein's concentration in each of the tissue sample lysates. Protein quantification of lysed ovaries was, therefore, determined using Bradford Assay (Bio-Rad Protein Assay Dye Reagent Concentrate, #5000006, Bio-Rad). This assay is built on the observation that Coomassie Brilliant Blue G-250 exists in two different colour forms, red (cationic) and blue (anionic). Under acidic conditions, the dye is in the red form ($Absorvance_{max}$=470 nm), and upon binding of the dye to proteins, it is converted into a stable unprotonated blue form (A_{max}=595 nm) [114,115].

To this aim, BSA (Albumin Bovine Fraction V, MB04602, Nzytech) was used to prepare a standard curve. Albumin samples were used at concentrations between 2.5 µg/mL and 50 µg/mL, and lysates were diluted 1:5 in distilled water. Bradford 5x was diluted to 2x in distilled water and added to the wells of both BSA standards and cell lysates. The mixture was carefully resuspended in the wells, and the absorbance of the protein-dye complex was measured at 595 nm wavelength using Tekan® multi-mode microplate reader. Protein samples, standards and blanks (consisting of cuvettes filled with water and dye reagent) were prepared in triplicate. The unknown sample concentration was determined using the standard curve.

III.8 Western Blotting

Western blotting is a technique commonly used for protein analysis that relies on the ability of an antibody to specifically bind to an antigen in a complex protein mixture.

Equal amounts of protein were mixed with sample buffer [final concentration of 0.625 M Tris-HCl pH 8.8, 2 % sodium dodecyl sulphate (SDS), 10 % glycerol, 1 M dithiothreitol (DTT) and 0.2 % bromophenol blue], heated in Thermoblock (Thermofisher) at 65 °C for 15 minutes, then at 95 °C for 5 minutes. Afterwards, samples were quickly placed in ice, to induce thermic shock. Samples were electrophoretically separated in a 10 % SDS–polyacrylamide gel, in LAEMMLI B running buffer [0.025 M Tris, 0.250 M glycin (MB01401, Nzytech), 0.0035 M SDS] with 30 mA amperage per gel. Afterward, samples were electrotransferred to nitrocellulose membranes in Tris-glycine transfer buffer (0.048 M Tris, 0.039 M glycin, 0.0012 M SDS and 20% methanol). The membrane and the gel were stacked as shown in **figure 10** (chromatography paper, GE Healthcare Life Sciences, Whatman®, 3 mm) and voltage was fixed in 30 V for 90 minutes. Following protein transference, membranes were washed in distilled water, stained with Ponceau S, and images were acquired in a ChemidocTM MP system (Bio-Rad). Then, membranes were washed in Tris-buffered saline (20 mM Tris pH 7.6

and 137 mM NaCl containing 0.1% Tris-Buffered Saline (TBS)-Tween 20), and they were blocked for 1 hour in 2.5 % non-fat dry milk in TBS-T. Primary antibodies diluted in BSA 2.5 % in TBS-T were incubated overnight at 4 °C with agitation (**table 2**). On the following day, membranes were washed with TBS-T for 30 minutes (TBS-T was changed every 10 minutes) and probed with the secondary antibody containing a HRP enzymatic tag (**table 2**) in BSA 2.5 % in TBS-T for 1 hour at room temperature, also with agitation (this step was not performed for IgGs detection, as the primary antibody was tagged with HRP enzyme). Blots were then washed with TBS-T for 30 minutes (TBS-T was changed every 10 minutes) and the signal was revealed with a chemiluminescent agent (luminol and peroxide solution, in a proportion of 1:2, #1705061, Bio-Rad) for 2 minutes at room temperature (**figure 11**). The reaction was visualized in a ChemidocTM MP imaging system. The Ponceau S staining was used for protein loading normalization, and quantification was performed using Image Lab software, version 4.0.1 (BioRad).

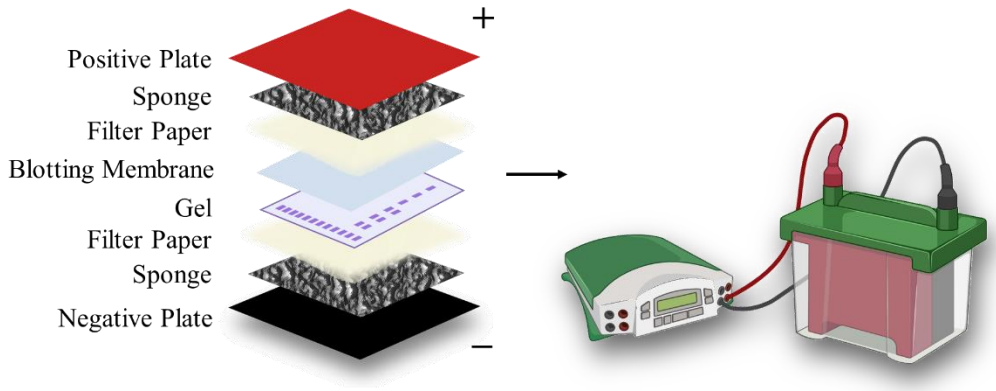


Figure 10: **Illustrative representation of gel and membrane stacking for transference step**. Adapted image. @Biorender.

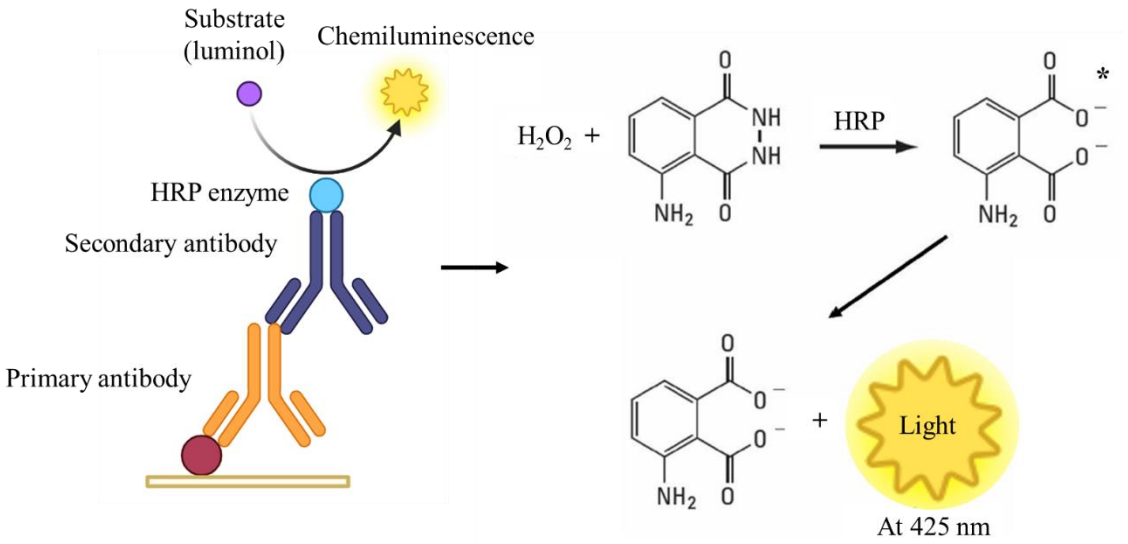


Figure 11: **Illustrative depiction of antigen detection by chemiluminescence.** HRP catalytic activity, promoting oxidation of substrates, such as luminol, by hydrogen peroxide, yielding a chemiluminescent byproduct. Adapted image. ©Biorender, ©2021 Thermo Fisher Scientific Inc, Western blotting Handbook.

Table 2: List of antibodies used for Western Blotting technique, and percentage of gel acrylamide for each detection.

Primary Antibodies	Secondary Antibody	Acrylamide %
Peroxidase-conjugated AffiniPure Donkey Anti-Mouse IgG 1:4000 715-035-150, Jackson ImmunoResearch	-	10 %
α-Actin (I-19) 1:1000 sc-1616, Santa Cruz Biotechnology	Peroxidase-conjugated AffiniPure Donkey Anti-Goat IgG 1:5000 715-035-150, Jackson ImmunoResearch	10 %

III.9 Statistical Analysis

Statistical analyses were performed with Excel programme (Microsoft® Excel® 64-bit, version 2103, Microsoft 365). Arithmetic means were given with a standard error of the mean (SEM). Unpaired student's t-test was used to compare between groups. $P < 0.05$ values were assumed to denote statistical significance: no symbol was used to denote $p > 0.05$; "*" was used for denoting $p < 0.05$, "**" for $p < 0.01$; "***" for $p < 0.001$ and "****" for $p < 0.0001$.

Chapter IV: Results

IV.1 Age-related Deposits in Ovarian Tissue

We performed SBB staining technique in groups of mice and rats aiming to understand the extent of ovarian lipofuscin accumulation during ovarian ageing. As aforementioned, SBB binds to lipids such as lipofuscin. **Figure 12** shows lipofuscin granules, marked as blue-black deposits, present in the stroma of reproductively aged mice and rats (**figure 12A** and **12B**, respectively).

Qualitatively, we observed that ovaries from the young mice (**figure 12A**, left) and rats (**figure 12A**, right), showed none or almost none SBB staining, in contrast to reproductively aged specimens, which were rich in SBB deposits. Graphs in **figures 12C** and **12D** show the quantitative results of SBB staining in ovaries from the mice and the rats' groups. We have observed that lipofuscin accumulation in the ovaries from reproductively aged mice was significantly higher than in ovaries from young mice (p-value <0.001): young mice, 0.28±0.21 %, compared to reproductively aged ones, 10.80±1.84 %. Regarding rats' group, lipofuscin accumulation in the ovaries of reproductively aged animals was, once again, significantly higher (p-value <0.001): young rats, 1.34±0.39 %, in contrast to reproductively aged ones 19.80±2.70 %.

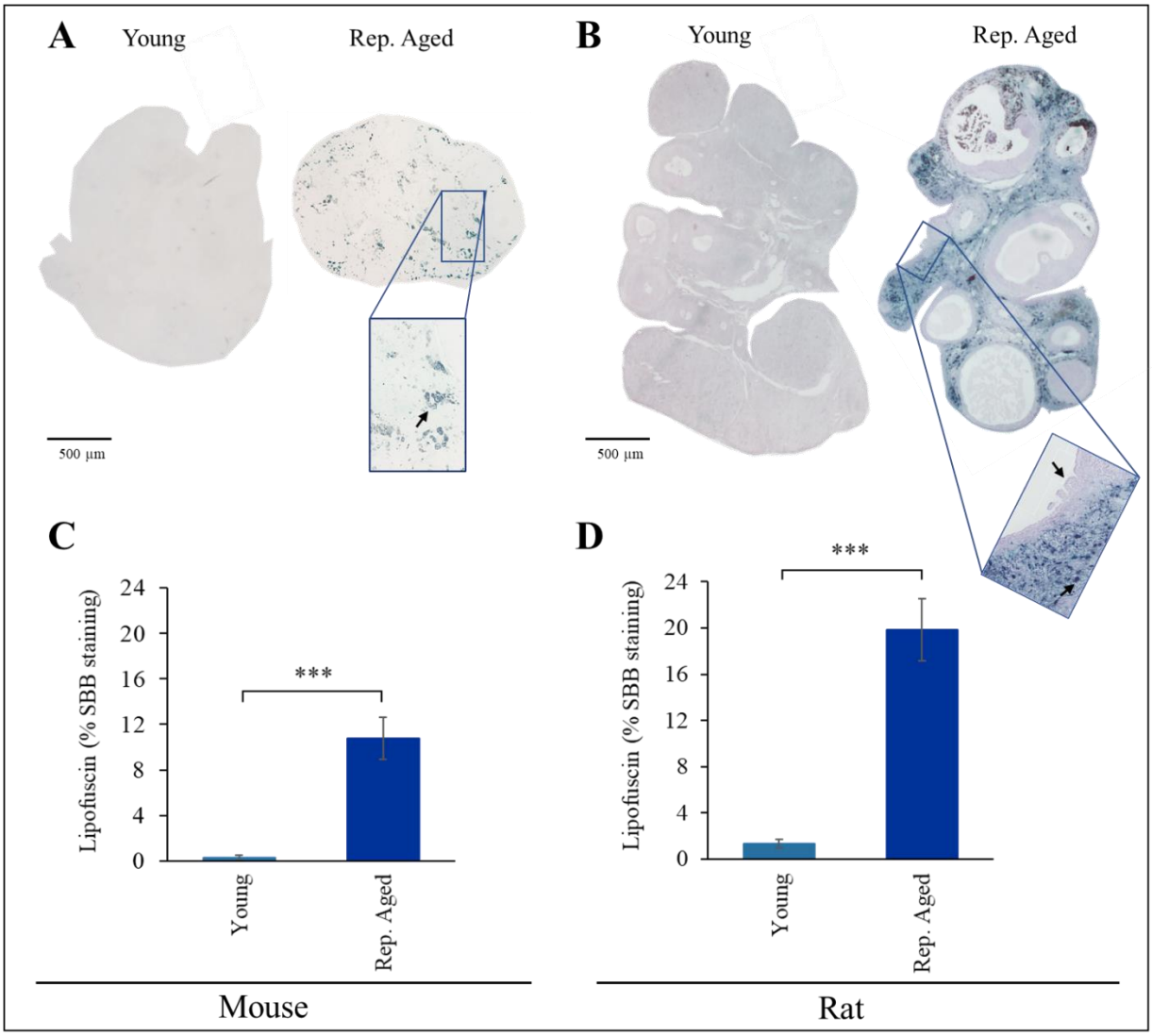


Figure 12: **Lipofuscin accumulation during ovarian ageing**. Mouse (left panel) and rat (right panel) results. **(A, B)** SBB staining of ovarian mid-sections of representative young and reproductively aged mice and rats, arrows evidencing SBB staining. **(C, D)** Graphical representations of the average values of lipofuscin accumulation for each animal and age group. Data is presented as a mean percentage of the total stained area over the total ovarian area ± SEM. *** P <0.001 for both mice and rat samples. Number of animals per group: young mice - n=5; reproductively aged mice - n=11; young rats - n=6, reproductively aged rats n=14.

IV.2 Age-related Accumulation of IgG in Ovarian Tissue

Considering the enhanced accumulation of cell senescence marker lipofuscin in reproductively aged groups of both species studied, we delved into bidirectional crosstalk between cellular senescence and chronic inflammation. To this aim, IHC was performed (**figure 8** and **table 1**), to assess IgG presence in the tissue and to identify the binding locations of these immunoglobulins. The results obtained revealed little to no immunostaining in the group of young mice and pronounced immunostaining in the group of reproductively aged mice (**figure 13A**). Quantitative measurements, depicted in **figure 13B**, clearly show the disparity in IgG

accumulation in the ovaries from young and reproductively aged mice (p-value <0.01): the mean percentage of ovarian immunostained area in young mice (0.041±0.026 %) was much lower compared with the mean percentage of ovarian immunostained area in reproductively aged mice (3.41±0.07 %).

Next, we quantified the expression of IgG heavy and light chains in the ovaries of mice (**figure 13C**). The group of reproductively aged animals was used as reference for normalization, because of the absence of signal for IgG light chain in some of the young animals. We observed significant differences in the amount of IgG expression between ovaries from young and reproductively aged mice. Ovaries from young mice revealed little or almost absent presence of IgG heavy and light chains [0.24±0.049 arbitrary units (a.u) and 0.0018±0.0018, respectively], contrasting with a clear presence of IgGs in the tissue of reproductively aged mice (**figure 13D**). The stacked bar chart denotes an increase (p-value <0.01) in the amount of IgGs expressed in ovarian tissue from reproductively aged mice compared to young ones. Interestingly, in a group of reproductively aged animals treated with apocynin, the age-related increase in ovarian IgG accumulation was significantly reduced (p-value <0.01), with 0.25±0.13 a.u. and 0.260±0.068 a.u. for light and heavy chain, respectively (**figure 13D**).

Afterward, the correlation between ovarian ageing and IgG accumulation was evaluated in rats (**figure 8** and **table 1**). In accordance with the IHC results obtained for mice, ovaries from young rats presented very little immunostaining when compared to reproductively aged animals (**figure 13E**). Quantitatively, the mean value for IgG presence in ovarian tissue of young rats (1.58±0.49 %) was significantly lower (p-value < 0.001) than in reproductively aged specimens (6.92±0.94 %). This disparity is graphically depicted in **figure 13F**.

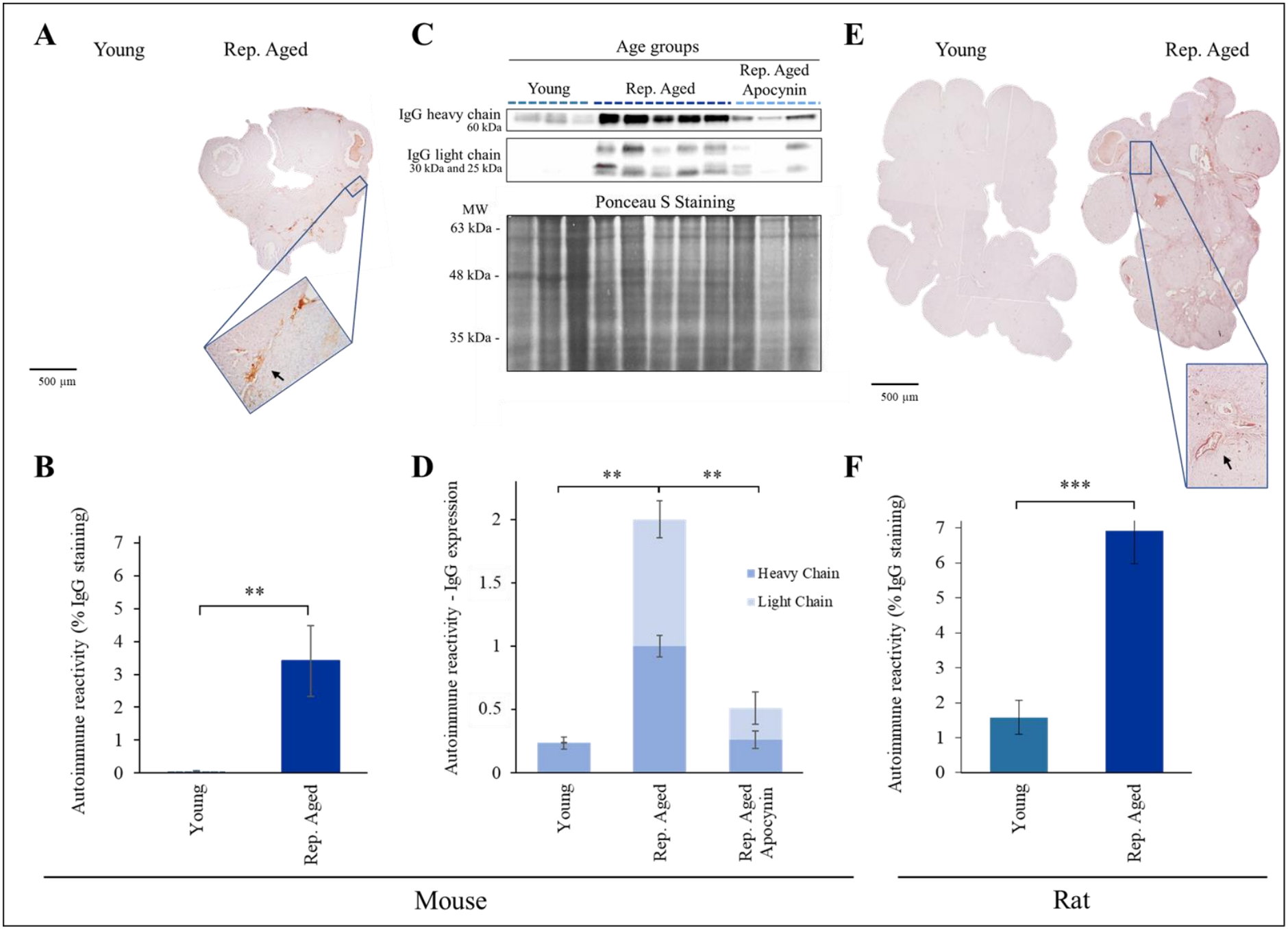

A
Young
Rep. Aged
500 µm
C
Age groups
Young
Rep. Aged
Rep. Aged Apocynin
IgG heavy chain 60 kDa
IgG light chain 30 kDa and 25 kDa
Ponceau S Staining
MW
63 kDa -
48 kDa -
35 kDa -
E
Young
Rep. Aged
500 µm
B
Autoimmune reactivity (% IgG staining)
**
Young
Rep. Aged
D
Autoimmune reactivity - IgG expression
**
**
Heavy Chain
Light Chain
Young
Rep. Aged
Rep. Aged Apocynin
F
Autoimmune reactivity (% IgG staining)
***
Young
Rep. Aged
Mouse
Rat

Figure 13: **IgG presence in the ovaries during reproductive ageing. (A)** Representative immunostaining of ovarian mid-sections of young and reproductively aged mice; the arrow points towards pronounced staining. **(B)** Graphical representation of the average values of immunostaining for each age group. Data is presented as a mean percentage of immunostained areas over the total ovarian areas ± SEM. **(C)** Detection of IgG chains' expression. Three sample groups are presented, relative to the expression in the reproductively aged group: young, reproductively aged and apocynin-treated reproductively aged mice. Ponceau image is displayed below, with molecular weights. **(D)** Graphical representation of IgG light and heavy chains expression. **(E)** Immunostaining of ovarian mid-sections of representative young and reproductively aged rats, as evidenced by the arrow. **(F)** Graphical representation of the average values of immunostaining for each age group; data quantification follows the same methodology as in (9B). ** P <0.01; *** P <0.001. Number of animals in IHC: young mice - n=7; reproductively aged mice - n=12; young rats - n=9, reproductively aged rats n=12. Number of mice in western blotting: young - n=3; reproductively aged - n=5; apocynin-treated reproductively aged - n=3.

IV.3 Evaluation of ovarian surface epithelium changes during reproductive ageing

Considering the results obtained so far, that revealed ovarian accumulation of markers of cellular senescence and increased IgG accumulation in ovaries from reproductively aged animals, we hypothesised that there could be associated cellular and morphological changes in these tissues.

Careful microscope observation of H&E-stained ovarian tissue allowed us to notice that the epithelia from reproductively aged mice and rats had an atypical morphology, with elongated cells (instead of cuboid), the presence of papillary growths and epithelium multilayers (**figures 14A and 14B**). Epithelial shedding was also observed.

Figures 14C and **14D** depict the quantification of abnormal epithelia. Results show that, in mice's group, the ovarian surface epithelium that was abnormal was significantly (p-value <0.05) increased in reproductively aged animals: 27.70±5.53 % of the total ovarian section perimeter had altered characteristics (**figure 14C**), contrasting with an average of 10.60±1.46 % of the total perimeter of the young group. Regarding the rat, we can observe in **figure 14D** that the young group showed an average abnormal ovarian perimeter of only 2.31±0.21 %. Once again, this bears a highly significant difference (p-value <0.0001) when compared to reproductively aged animals, that presented an abnormal epithelial mean of 45.3± 2.45 %.

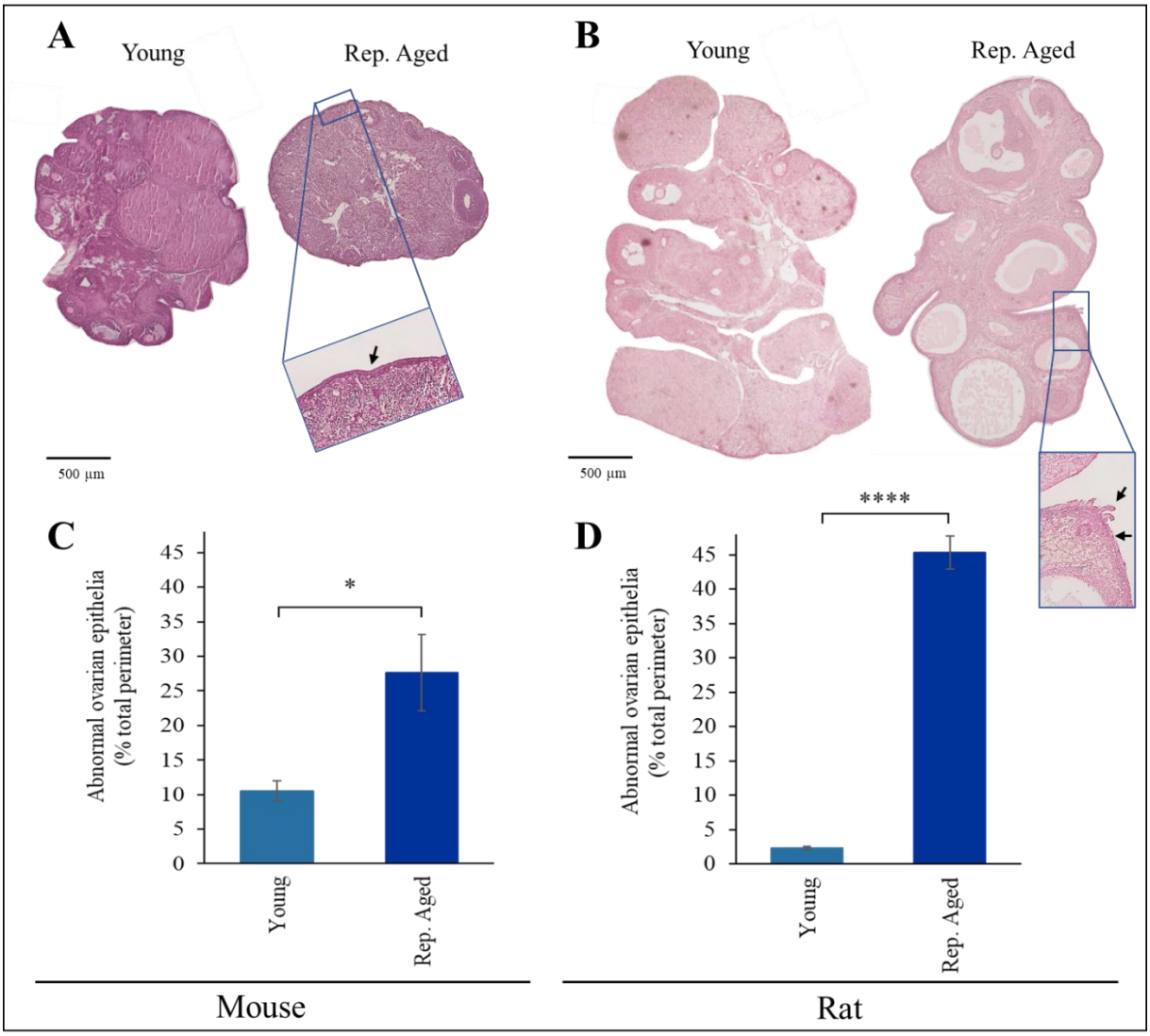


Figure 14: **Abnormal surface of ovarian surface epithelium**. **(A, B)** Representative H&E staining of ovarian mid-sections of young and reproductively aged mice and rats, revealing a contrast in epithelial morphology, namely elongated morphology and papillary growths, pointed by arrows. **(C, D)** Graphical representations of the average values of the quantified abnormal epithelia for each group. Data is presented as a mean percentage of the ratio of length of abnormal perimeter measured over the total ovarian section perimeter ± SEM. * P <0.05; **** P <0.0001. Number of animals per group: young mice - n=5; reproductively aged mice - n=9; young rats - n=6; reproductively aged rats - n=12.

IV.4 Fibroblast-like Stromal Cells Biomarker

Previous studies have demonstrated that reproductive ageing entails fibrosis formation in the ovary [28,30]. In the context of epithelium morphology alterations and neoplasm development it is known that fibroblasts and myofibroblasts, positive for α-SMA, play crucial roles in age-associated ovarian fibrosis and stromal changes, and progression of tumour cells is followed by alterations in cell composition and ECM [105]. The stroma of ovarian epithelial tumours reveals α-SMA great expression, suggesting stromal stimulation mediated by neoplastic epithelium [106]. In addition, tumour cells of serous and clear cell ovarian carcinoma

exhibit α-SMA positive expression [105]. Therefore, we proceeded to the evaluation of α-SMA expression patterns of in young and reproductively aged mice.

The expected molecular weight for α-SMA is 45 kDa. However, additional bands of approximately 60 and 63 kDa were present in the blot. Interestingly, these bands were only observed in the groups of reproductively aged mice and apocynin-treated reproductively aged mice. At the expected molecular weight, we observed a significant age-related decrease (p-value <0.1) of α-SMA in reproductively aged mice (1±0.15 a.u), when compared to young mice (2.17±0.18 a.u), as shown in **figure 15**. Apocynin-treated group presented no signal at all, a significant decrease in comparison with the values of young mice (p-value <0.01) as well as with reproductively aged mice (p-value <0.1).

Regarding the bands 60 and 63 kDa we verified a significant increase (p-value <0.5) with ageing: young mice group presented no signal, in contrast to the values of 1±0.26 a.u, of reproductively aged mice (**figure 15**). The apocynin-treated group presented a significant increase comparing to young mice (p-value <0.5), with a mean value of 1.15±0.34 a.u. and revealed no differences when compared to reproductively aged mice.

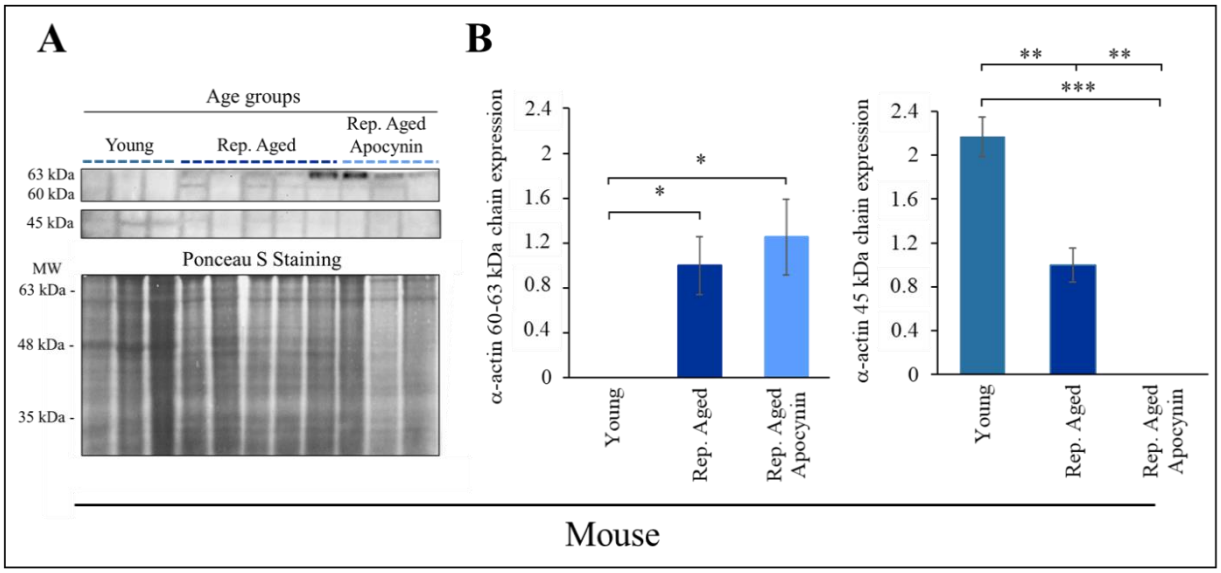


Figure 15: **α-SMA expression in mice's ovaries. (A)** Three sample groups are presented in the blot: young, reproductively aged and apocynin-treated reproductively aged mice. The bands depicted in the blot correspond to molecular weights of 45, 60 and 63 kDa. Ponceau image is displayed below, with molecular weights. **(B)** Graphical representation of α-SMA relative expression. The data is presented relative to the expression in the reproductively aged group ± SEM**.** Left: sum of 60 and 63 kDa band signals between reproductively aged and apocynin-treated reproductively aged and young mice. * P <0.05; * P <0.01; *** P <0.001. Number of mice: young - n=3; reproductively aged - n=5; apocynin-treated reproductively aged - n=3.

IV.5 Influence of Parity in Ovarian Ageing

The monthly cycles of ovulation are part of ovarian dynamic. This process involves an intricate interplay between follicular rupture, disruption and remodelling of ECM and ovarian surface epithelium [2,14]. It is known that ovulations promote an increase in ovarian wound healing processes and that they are associated with a higher risk of developing ovarian cancer

[116]. The mechanisms behind this have not yet been elucidated; therefore, we proceeded to evaluate some of the previously studied parameters (accumulation of deposits in ovarian tissue, expression of IgGs, ovarian surface epithelium abnormalities) in ex-breeder (multiparous) mice, which have undergone fewer ovulatory cycles than nulliparous ones.

To assess lipofuscin accumulation, SBB staining was performed. We observed that multiparous mice presented less SBB staining (p-value <0.05), with a mean stained area of 3.46±1.84 %, in contrast to nulliparous mice, which presented a mean stained area of 10.70±0.21 % (**figure 16A)**. To determine if IgG presence in the ovaries was affected by parity, IHC assays were conducted (**table 1 and figure 8**). Immunostaining quantification in did not denote statistical differences: **figure 16B** depicts a mean IgG-stained area of 3.41±1.08 % for nulliparous mice and 0.61±0.13 % for multiparous ones. Lastly, to evaluate ovarian epithelium surface abnormalities, we carefully observed ovarian tissue under an optical microscope. We note that both nulliparous and multiparous groups presented elongated cells, surface papillary growths and clefts (27.60±5.53 % and 25.0±3.8 %, respectively), albeit not presenting significant differences between groups (**figure 16C)**.

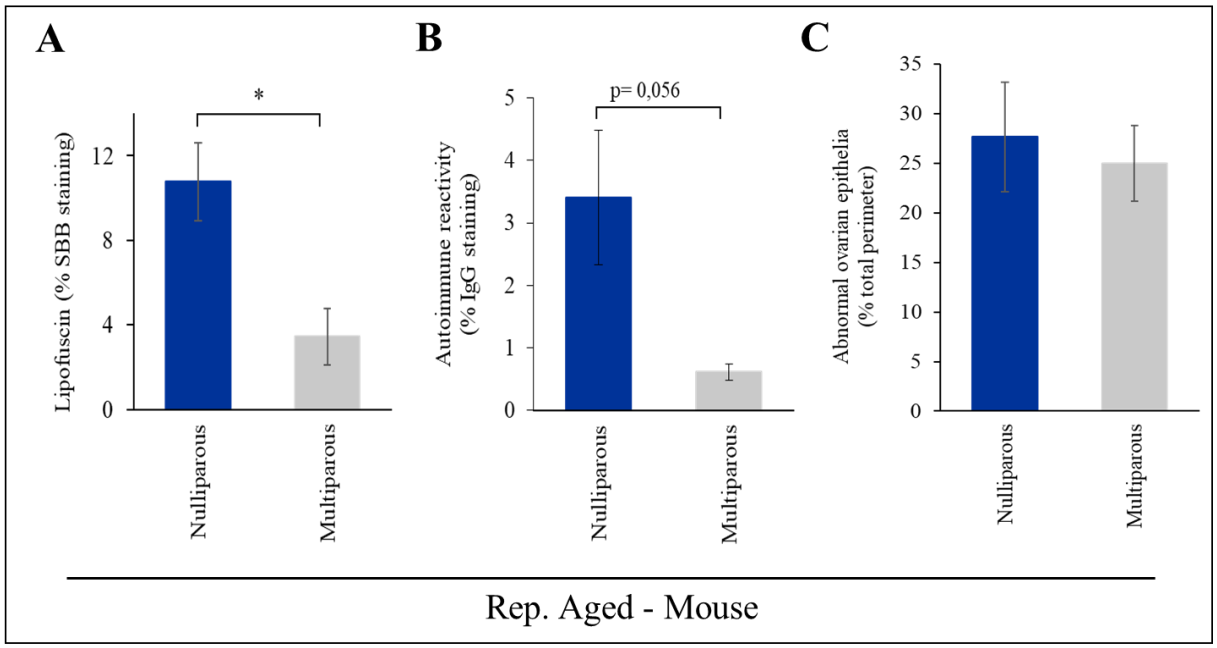


Figure 16: **Influence of parity in ovarian ageing**. Graphical representations of the results obtained from analysis of ovarian mid-sections from nulliparous and multiparous reproductively aged mice. **(A) Lipofuscin accumulation during ovarian ageing**. Data is presented as a mean percentage of the stained area over the total ovarian area. **(B) IgG presence during ovarian ageing**. Data is presented as a mean percentage of immunostained area over the total ovarian area ± SEM. **(C) Quantified length of abnormal ovarian surface epithelium**. Data is presented as a mean percentage of the calculated abnormal perimeter over the total ovarian perimeter. * P <0.05. Number of mice in lipofuscin accumulation quantification: nulliparous - n=6; multiparous - n=5. Number of mice in IgG quantification: nulliparous - n=7; multiparous - n=5. Number of mice in abnormal ovarian epithelium surface quantification: nulliparous - n=6; multiparous - n=3.

Chapter V: Discussion

In females, the reproductive system, including the ovaries, ages faster than most other organs, resulting in hormonal changes at a relatively early age, loss of fertility, and the onset and development of pathologies such as skin atrophy and accelerated skin ageing (collagen, wrinkles, and dryness), reduction of endothelial-dependent vascular function in the cardiovascular system, due to oestrogen deficiency, as well as development of osteoporosis due to bone loss and articular cartilage degeneration. [117,118]. During ovarian ageing, a unique population of multinucleated stromal cells, positive for macrophage markers, has been identified as an ovarian ageing hallmark [28,59-62]. These cells, MNGCs, are characterized by a large size, often displaying a pale, light brown cytoplasm with a foamy appearance [28]. They have been previously described in ovaries collected from reproductively aged female mice, goats, and sheep [30,73]. These cells were shown to accumulate lipofuscin, a marker that is associated with cellular senescence [84]. Previous studies demonstrated that MNGCs may contribute to ovarian ageing, by increasing the levels of ROS and inflammation [119-121].

In the present study, it was observed that ovaries from reproductively aged rats exhibited enhanced lipofuscin accumulation. Ovarian tissues from both mice and rats also presented an age-related increase in IgG accumulation, and, when treated with apocynin, its levels decreased to values commonly seen in juvenile mice. These changes were accompanied by papillary projections of the epithelial cell lining of the ovaries of reproductive aged mice and rats. In addition, alterations in expression of α-SMA protein were found in western blotting, presenting additional bands with higher molecular weights (63 kDa) in ovaries from reproductively aged mice and an age-related decrease of 45 kDa α-SMA. Lastly, our results indicate a trend towards increased lipofuscin accumulation in nulliparous mice compared to multiparous mice.

Numerous biological processes are being identified as biomarkers to characterise senescent cells in tissues. Lipofuscin, for instance, has been considered a crucial cellular senescence hallmark [84]. Using SBB staining technique, we were able to confirm other authors findings that have observed an increased accumulation of insoluble lipids, namely lipofuscin, in ovaries collected from reproductively aged mice and rats, contrasting with ovaries collected from young animals [35,68,122]. Also, our results align with the already described increased presence of lipofuscin deposits in ovaries from reproductively aged mice, murine, goats, and sheep [30,35,73,123].

Several studies revealed that presence of lipofuscin deposits is correlated with the presence of MNGCs [30,35,73,123]. Emerging evidence suggests that MNGCs may exhibit features characteristic of cellular senescence, including the aforementioned lipofuscin accumulation, increased expression of senescence-associated markers such as p16, p21, and SA-β-gal [35,62,67,68]. Lipofuscin accumulation holds a pathogenic and cytotoxic role due to its capacity to incorporate increased amounts of transition metals (iron), leading to a redox-active surface and ROS generation, and affecting pathways necessary to remove oxidized products, promoting enhanced OS and damage in the tissue [119,120]. The results obtained in this study suggest that the abundant presence of the senescence hallmark lipofuscin in reproductively aged rats' ovaries might correspond to an increase in MNGCs population.

Polyploid/multinucleated cancer cells have been identified in many types of malignant tumours, for instance melanoma, non-small-cell lung cancer, glioblastomas or ovarian cancer,

but the presence of MNGCs with a senescent-like phenotype has not yet been described in association with tumours [59-62,128-130]. However, recent studies non-small-cell-lung carcinomas showed that tumours high number of cancer cells with lipofuscin accumulation are clinically more aggressive [84]. In the ovarian cancer context, Leydig cells in Sertoli-Leydig cell tumour were shown to have lipofuscin accumulation [84,85]. The accumulation of lipofuscin in cancer cells could indicate that the observed presence of lipofuscin in ovaries from reproductively aged rats and mice, in this study, may suggest a potential link to neoplastic lesions.

In the current study, the increased burden in senescent markers was found to be consistent with age-related increased accumulation of IgGs in ovarian tissues from both mice and rats. Western blotting also revealed little to no presence of IgG heavy and light chains in young mice in comparison to the presence of IgG chains in the tissue of reproductively aged mice. In the normal functioning of the immune system, IgGs are secreted by plasma cells, a type of differentiated B lymphocyte, to enhance the process of opsonization, facilitating the engulfment of pathogens by phagocytes (as well as to activate the complement system) [124]. Interestingly, Qiu et al. reported that in malignant settings, namely in tissue derived from epithelial tumours (liver, colon, breast and lung) there was an increased expression of cancer-related IgG, in which metastasized samples had increased abundance than matched primary tumours [125]. The same author showed that the presence of cancer-related IgG is associated with cancer cells' high proliferation, invasion and colony formation capacity [125]. Similar cellular deposits of IgGs were observed in 80% of papillary thyroid carcinoma cases, when compared with other thyroid lesions that did not present tissue IgG deposits [126]. Considering that cancer is often associated with extreme oxidative and inflammatory environments, IgG accumulation seems to be increased in tissues with high levels of oxidative and inflammatory stress, common features of aged tissues and cancer [108].

Recent research demonstrated that IgG accumulation in white adipose tissue during ageing disrupts its normal functioning and precedes macrophage recruitment, activating macrophages through Ras signalling pathway and inducing adipose tissue fibrosis. Moreover, it was shown that preventing IgG accumulation in aged tissues prolongs health and lifespan [127]. Although the mechanisms behind IgG accumulation and macrophage presence are not thoroughly understood, it seems that there might be a correlation between these components. Another recent study has suggested that IgG glycome is an important contributor to the process of ageing, revealing that glycans attached to IgG change with age and disease, and are key regulators of chronic systemic inflammation, one of the main drivers of ageing and age-related diseases [128]. The proposed mechanism is that, as people age, glycans that suppress inflammation are being replaced with inflammation-promoting glycans [128]. However, the rate of this conversion highly depends on individual responses, being modulated by genetic, epigenetic, and environmental factors [128].

Treatment with the antioxidant and anti-inflammatory drug apocynin seems to play a protective role, preventing IgG accumulation in ovarian tissues and being capable of restoring IgG levels in ovaries from reproductively aged mice to levels normally observed in younger mice [129]. Apocynin inhibits NOX-mediated conversion of oxygen (O_2) to superoxide (O_2^-),

reducing the production of ROS and, therefore, impairing OS [30,130]. A study on hepatic inflammation in non-alcoholic steatohepatitis has shown that OS was associated with the development of IgG against antigens originating from peroxidation products, suggesting that IgG might influence disease evolution by antibody-mediated injury [131]. Due to apocynin's antioxidant properties, its administration might impair the setting of OS, and, therefore, delay production of IgG and, subsequently, delay the recruitment of immune cells to tissues, namely macrophages. Our results with apocynin confirmed the potential of this treatment in the prevention of tissue ageing features and a potential prevention of neoplastic lesions.

The aforementioned results were accompanied by an increase in ovarian surface epithelium abnormalities. Ovaries collected from reproductively aged mice and rats showed an atypical cellular lining, with elongated cells (instead of cuboid), arranged in a pseudostratification (instead of the typical single layer), and the presence of papillary-like epithelial proliferations. These modifications were observed in ovaries with high accumulation of lipofuscin. When we quantified and compared the morphology of the cellular lining of ovaries from young and reproductively aged groups, significant differences were observed between these groups. These alterations have also been reported by other researchers, and were linked to the ovulation process [2].

Ovulation is a process that involves an extensive disruption and remodelling of the ovarian surface epithelium [132]. It triggers wound healing processes, including tissue remodelling mechanisms, angiogenesis, and inflammatory responses that requiring the recruitment of great populations of immune cells [35,132]. Extracellular matrix and ovarian surface epithelium are capable of repairing themselves, despite extensive remodelling to which they are subjected [14]. However, it has been described that, with advancing age, ovarian surface epithelium's wound repair efficiency is compromised: in reproductively old mice, both *in vivo* and *in vitro*, it was observed increased epithelial thickness, invaginations into the stroma, and epithelial outgrowths [2]. Moreover, in reproductively aged mice and women, OSE revealed cell hyperplasia and stratified growth, papillary growth, invaginations into the stroma, and inclusion cysts [133]. These observations are consistent with our although we did not clearly identify invaginations into the stroma, and the presence of inclusion cysts was not detected. There are numerous factors that could account for the failure of remodelling processes. A potential mechanism responsible for these phenotypes may be dysregulation of the EMT [2]. Its dysregulation may lead, ultimately, to a metaplastic wound repair due to cellular acquisition of mesenchymal traits and undifferentiated phenotype [21,24,25,134-138].

Regarding the relationship between the observed abnormalities in ovarian surface epithelium morphology and ovarian cancer, there are contradictory reports on the occurrence of histological changes in normal ovaries from healthy women that were removed by prophylactic oophorectomy with histories of familial ovarian cancer. Some studies indicate increased papillomatosis, pseudostratification and invaginations in the ovarian surface epithelium, as well as the presence of inclusion cysts and in ovaries, while others demonstrated only nuclear changes in the OSE of such women [139-142]. However, presence of ovarian surface epithelial alterations and inclusion cysts has been observed in several mouse models for ovarian tumours [97,143-145]. This suggests a possible relationship with the onset of preneoplasms.

Age-associated fibrosis has been reported in the ovarian stroma of mice and murine, being characterized by excess collagen deposition in the ECM, particularly collagen I and III, by myofibroblasts (the activated form of fibroblasts) [2,18,28,30,35,54,103,104,121,146-148]. Age-related fibrosis has been linked to tissue dysfunction and occurs in several organ systems, including the ovary, compromising the regulation of ECM remodelling [2,28]. α-SMA indicates fibroblast activation and its age-related accumulation in ovarian stroma is described to be a stimulus for macrophage fusion [18,35,54,121,146,147]. Briley *et al.* have described MNGCs frequent presence in the vicinity of cells that stain positive for α-SMA, which suggests that the age-associated penetrance of MNGCs in the ovaries may be explained by an attempt to clear excessive deposition of debris and collagen in the ovary, generated by repeated cycles of ovulation, *CL* involution and wound healing [18,28]. In light of this and the enhanced alterations in ovarian surface epithelium, we focused on studying age-related α-SMA modifications that occur in matrix remodelling.

Alterations in the expression pattern of α-SMA were found, namely the appearance of additional western blotting bands with higher molecular weight (60-63 kDa) than the expected for α-SMA (45 kDa) in ovaries from reproductively aged mice; the presence of α-SMA 45 kDa band was clear in young mice but diminished in reproductively aged animals. Treatment with apocynin did not revert the tendencies observed in α-SMA expression. It has been reported that actin forms aggregates during ageing, which may explain why young mice did not present 60-63 kDa bands, while reproductively aged mice had [149]. Additional studies must be performed to allow quantification of total α-SMA, regardless of its size, such as dot blot, in order to verify the putative existence of bands with higher molecular weight. Moreover, previous observations by our group revealed that treatment of ovaries from reproductively aged mice with apocynin reduced the levels of fibrosis [30].

Regarding a possible link between α-SMA presence and predisposition for ovarian neoplasms, it is known that progression of tumour cells is followed by alterations in cell composition and ECM, and that the stroma of ovarian epithelial tumours reveals α-SMA great expression, suggesting stromal stimulation mediated by neoplastic epithelium [105,106]. For instance, tumour cells of serous and clear cell ovarian carcinoma have α-SMA expression [105].

Ovulation has been suggested as a contributing factor in ovarian ageing by several research works, including the current study [117,150-153]. Hence, there was interest in exploring further whether parity plays a protective role among all the aforementioned alterations. In this regard, it was used a mice model which had been subjected to less ovulations along its reproductive lifespan–multiparous mice–an animal model that was already utilized by Urzua *et al.* for ovary ageing study [120]. Since these female mice are used to maintain colonies, and because they are subjected to consecutive pregnancies, during which ovulations do not occur, the number of ovulations undergone throughout their lifetime is diminished.

It was assessed the accumulation of senescence marker lipofuscin, IgG antibodies, and epithelium abnormalities in ovaries from nulliparous reproductively aged mice and multiparous reproductive aged mice. Our findings revealed that the only alteration observed concerned lipofuscin accumulation, implying increased MNGCs content in ovaries from nulliparous mice,

as opposed to those from multiparous mice. These results are corroborated by previous works by Urzua *et al.*, who described differential accumulation of lipofuscin in nulliparous mice, and correlated it with increased levels of NF-κB DNA damage [120]. The observed differences in lipofuscin accumulation goes according to the hypothesis that ovaries age more rapidly when subjected to incessant ovulations, since the inflammatory events and OS responses that accompany a successful ovulation render the ovaries more susceptible to damage [119,153].

The absence of significant differences in the presence IgG can be due to the fact that, although the number of ovulations in multiparous mice was lower, ovulations continued to occur. In the future, it will be interesting to use a model in which a contraceptive is administered for most of the animal's life to further understand the effect of ovulation suppression, considering that the use of oral contraceptives has been reported to mitigate age-related ovarian ageing [154]. Alternatively, a superovulation model, similar to the one used by Nie *et al.*, could be used to determine if there would be an increase in the accumulation of MNGCs and IgGs, given that it was stated that this intervention in mice lead to increased OS damage products [155]. Regarding the lack of differences in present abnormalities in the ovarian epithelium, we may find that lipofuscin might play a dominant role in inducing epithelial abnormalities in both animal models, due to chronic stress and mutation induction, overshadowing the protective effects of reduced ovulations in multiparous animals. Additionally, the fact that the observed results were seen only in MNGCs accumulation may indicate the sequence of events that occurs during ovarian ageing.

Chapter VI: Conclusion and Future Perspectives

The present study revealed that, during mice's and rats' reproductive ageing, the ovary undergoes and molecular changes, demonstrating increased content in senescence hallmark lipofuscin that paralleled with enhanced presence of IgG. These results showed a close relationship with the age-related appearance of abnormalities in ovarian surface epithelium, as well as composition changes in ECM, which may reflect the onset of pathophysiological processes. In addition, it showed that reduced ovulations hold protective effects against lipofuscin accumulation in the ovaries.

Considering apocynin's role in diminishing IgG accumulation, additional studies with apocynin administration and comparison of the ovarian surface epithelium morphology of ovaries may allow us to perceive whether this treatment would impair the age-related development of morphology alterations. Moreover, it would be important to characterise the expression of mesenchymal markers [N-cadherin (cadherin switch), vimentin, or galectin-1, whose upregulation induces metastasis in epithelial ovarian cancer] in epithelial cells that reveal alterations, exploring the association between the observed morphology alterations and EMT dysregulation [25,156,157].

List of Figures & Tables

Figures

Figure 1: Ovarian histology and different stages of follicle maturation. Diagram of a sectioned ovary, picturing different stages of follicle maturation, ovulation and luteal phase.

Figure 2: Diagrammatic representation of the different phases of the ovarian cycle and main regulatory hormones, ovarian and pituitary. Image adapted from Mendes, S. *et al*, "New Insights into the Process of Placentation and the Role of Oxidative Uterine Microenvironment" and Timoteo-Ferreira, F *et al*, "Redox imbalance in age-related ovarian dysfunction and perspectives for its prevention".

Figure 3: Post-ovulatory wound healing. Acute wounds progress through the phases of inflammation, proliferation, and remodelling, depicted, respectively, in A-C images. (A) Pro-inflammatory macrophages are recruited to phagocytise dead cells and debris, and secrete inflammatory cytokines (tumour necrosis factor-α, IL-6 and IL-1β), vascular permeability factors, and proteases that enhance the recruitment of immune cells into the wound. (B) Cells from the vicinity of the wound and epithelium migrate into the wound, and new blood vessels now populate the area. The dividing fibroblasts deposit collagen and shift the wound microenvironment from the inflammatory to the growth state. Pro-wound healing macrophages are present, secreting factors that aid in angiogenesis, collagen deposition, and re-epithelialization. (C) Macrophages secrete MMPs to aid cellular migration and maturation of collagen, and engulf excessive ECM, to return tissue homeostasis. Unregulated deposition of ECM can lead to fibrosis [12,15,18].

Figure 4: Process and pathogenesis of organ fibrosis. Damage caused by various stimuli, such as ageing, trauma or inflammation, lead to the release of cytokines and growth factors to induce fibroblast activation and generation of temporary ECM for the regeneration of injured tissues. Persistent damage and inflammation cause excessive accumulation of ECM, ultimately leading to tissue fibrosis. Image adapted from Yang *et al*, "Aryl hydrocarbon receptor: From pathogenesis to therapeutic targets in aging-related tissue fibrosis".

Figure 5: The basic components of the innate and adaptive immune responses. Image from Mehta, K. *et al*, Immunotherapy in genitourinary malignancies.

Figure 6: Potential causal factors and hallmarks of cellular senescence. Senescence is a damage response to cellular stressors such as DNA damage, mitochondrial dysfunction, oxidative stress, inflammation, or oncogene activation. The damage responses activated lead to enhanced expression of p21 and p16, aberrant cell morphology, loss of lamin B1, and increased SA-β-gal activity [69-71].

Figure 7: Simplified diagram of the experimental animal set-up used in this study, describing the number and age of the studies animals. "Rep. Aged" is the abbreviation for "Reproductively Aged". (A) Depicts the set-up used in staining and IHC techniques. (B) Depicts the set-up for western blotting, in which all reproductive aged mice were nulliparous.

Figure 8: Schematic image of IHC procedure. Antibodies raised in the same species as the target tissue were chosen, allowing cross-reactivity and detection of IgG in the tissue.

Figure 9: Representative images of ovarian mid-sections depicting the measurement methods in Image J software. (A) Threshold cut point determination used for SBB staining relative quantification. (B) Threshold cut point determination used for IgG staining relative quantification. (C) Perimeter considered abnormal used for relative quantification. The ovaries presented were collected from two rep. aged rats (A and C), and a rep. aged mouse (B).

Figure 10: Illustrative representation of gel and membrane stacking for transference step. Adapted image. @Biorender.

Figure 11: Illustrative depiction of antigen detection by chemiluminescence. HRP catalytic activity, promoting oxidation of substrates, such as luminol, by hydrogen peroxide, yielding a chemiluminescent byproduct. Adapted image. ©Biorender, ©2021 Thermo Fisher Scientific Inc, Western blotting Handbook.

Figure 12: Lipofuscin accumulation during ovarian ageing. Mouse (left panel) and rat (right panel) results. (A, B) SBB staining of ovarian mid-sections of representative young and reproductively aged mice and rats, arrows evidencing SBB staining. (C, D) Graphical representations of the average values of lipofuscin accumulation for each animal and age group. Data is presented as a mean percentage of the total stained area over the total ovarian area ± SEM. *** $P < 0.001$ for both mice and rat samples. Number of animals per group: young mice - n=5; reproductively aged mice - n=11; young rats - n=6, reproductively aged rats n=14.

Figure 13: IgG presence in the ovaries during reproductive ageing. (A) Representative immunostaining of ovarian mid-sections of young and reproductively aged mice; the arrow points towards pronounced staining. (B) Graphical representation of the average values of immunostaining for each age group. Data is presented as a mean percentage of immunostained areas over the total ovarian areas ± SEM. (C) Detection of IgG chains' expression. Three sample groups are presented, relative to the expression in the reproductively aged group: young, reproductively aged and apocynin-treated reproductively aged mice. Ponceau image is displayed below, with molecular weights. (D) Graphical representation of IgG light and heavy chains expression. (E) Immunostaining of ovarian mid-sections of representative young and reproductively aged rats, as evidenced by the arrow. (F) Graphical representation of the average values of immunostaining for each age group; data quantification follows the same methodology as in (9B). ** $P < 0.01$; *** $P < 0.001$. Number of animals in IHC: young mice - n=7; reproductively aged mice - n=12; young rats - n=9, reproductively aged rats n=12. Number of mice in western blotting: young - n=3; reproductively aged - n=5; apocynin-treated reproductively aged - n=3.

Figure 14: Abnormal surface of ovarian surface epithelium. (A, B) Representative H&E staining of ovarian mid-sections of young and reproductively aged mice and rats, revealing a contrast in epithelial morphology, namely elongated morphology and papillary growths, pointed by arrows.

(C, D) Graphical representations of the average values of the quantified abnormal epithelia for each group. Data is presented as a mean percentage of the ratio of length of abnormal perimeter measured over the total ovarian section perimeter ± SEM. * P <0.05; **** P <0.0001. Number of animals per group: young mice - n=5; reproductively aged mice - n=9; young rats - n=6; reproductively aged rats - n=12.

Figure 15: α-SMA expression in mice's ovaries. (A) Three sample groups are presented in the blot: young, reproductively aged and apocynin-treated reproductively aged mice. The bands depicted in the blot correspond to molecular weights of 45, 60 and 63 kDa. Ponceau image is displayed below, with molecular weights. (B) Graphical representation of α-SMA relative expression. The data is presented relative to the expression in the reproductively aged group ± SEM. Left: sum of 60 and 63 kDa band signals between reproductively aged and apocynin-treated reproductively aged and young mice. * P <0.05; * P <0.01; *** P <0.001. Number of mice: young - n=3; reproductively aged - n=5; apocynin-treated reproductively aged - n=3.

Figure 16: Influence of parity in ovarian ageing. Graphical representations of the results obtained from analysis of ovarian mid-sections from nulliparous and multiparous reproductively aged mice. (A) Lipofuscin accumulation during ovarian ageing. Data is presented as a mean percentage of the stained area over the total ovarian area. (B) IgG presence during ovarian ageing. Data is presented as a mean percentage of immunostained area over the total ovarian area ± SEM. (C) Quantified length of abnormal ovarian surface epithelium. Data is presented as a mean percentage of the calculated abnormal perimeter over the total ovarian perimeter. * P <0.05. Number of mice in lipofuscin accumulation quantification: nulliparous - n=6; multiparous - n=5. Number of mice in IgG quantification: nulliparous - n=7; multiparous - n=5. Number of mice in abnormal ovarian epithelium surface quantification: nulliparous - n=6; multiparous - n=3.

Tables

Table 1: List of antibodies used for IHC technique.

Table 2: List of antibodies used for Western Blotting technique, and percentage of gel acrylamide for each detection.

.

References

1. Mescher, A.L. *Junqueira's Basic Histology : Text and Atlas*, 16th ed.
2. Mara, J.N.; Zhou, L.T.; Larmore, M.; Johnson, B.; Ayiku, R.; Amargant, F.; Pritchard, M.T.; Duncan, F.E. Ovulation and ovarian wound healing are impaired with advanced reproductive age. *Aging (Albany NY)* **2020**, *12*, 9686-9713, doi:10.18632/aging.103237.
3. Caligioni, C.S. Assessing reproductive status/stages in mice. *Curr Protoc Neurosci* **2009**, *Appendix 4*, Appendix 4I, doi:10.1002/0471142301.nsa04is48.
4. Tan, O.L.; Fleming, J.S. Proliferating cell nuclear antigen immunoreactivity in the ovarian surface epithelium of mice of varying ages and total lifetime ovulation number following ovulation. *Biol Reprod* **2004**, *71*, 1501-1507, doi:10.1095/biolreprod.104.030460.
5. Chen, H.L.; Marcinkiewicz, J.L.; Sancho-Tello, M.; Hunt, J.S.; Terranova, P.F. Tumor necrosis factor-alpha gene expression in mouse oocytes and follicular cells. *Biol Reprod* **1993**, *48*, 707-714, doi:10.1095/biolreprod48.4.707.
6. Jabbour, H.N.; Sales, K.J.; Catalano, R.D.; Norman, J.E. Inflammatory pathways in female reproductive health and disease. *Reproduction* **2009**, *138*, 903-919, doi:10.1530/REP-09-0247.
7. Roby, K.F.; Weed, J.; Lyles, R.; Terranova, P.F. Immunological evidence for a human ovarian tumor necrosis factor-alpha. *J Clin Endocrinol Metab* **1990**, *71*, 1096-1102, doi:10.1210/jcem-71-5-1096.
8. Miller, B.H.; Takahashi, J.S. Central circadian control of female reproductive function. *Front Endocrinol (Lausanne)* **2013**, *4*, 195, doi:10.3389/fendo.2013.00195.
9. Stocco, C.; Telleria, C.; Gibori, G. The molecular control of corpus luteum formation, function, and regression. *Endocr Rev* **2007**, *28*, 117-149, doi:10.1210/er.2006-0022.
10. Block, E. Quantitative morphological investigations of the follicular system in women; variations in the different phases of the sexual cycle. *Acta Endocrinol (Copenh)* **1951**, *8*, 33-54, doi:10.1530/acta.0.0080033.
11. Yuan, W.; Giudice, L.C. Programmed cell death in human ovary is a function of follicle and corpus luteum status. *J Clin Endocrinol Metab* **1997**, *82*, 3148-3155, doi:10.1210/jcem.82.9.4191.
12. Zaniker, E.J.; Babayev, E.; Duncan, F.E. Common mechanisms of physiological and pathological rupture events in biology: novel insights into mammalian ovulation and beyond. *Biol Rev Camb Philos Soc* **2023**, *98*, 1648-1667, doi:10.1111/brv.12970.
13. Zhang, Z.; Huang, L.; Brayboy, L. Macrophages: an indispensable piece of ovarian health. *Biol Reprod* **2021**, *104*, 527-538, doi:10.1093/biolre/ioaa219.
14. Xu, J.; Zheng, T.; Hong, W.; Ye, H.; Hu, C.; Zheng, Y. Mechanism for the Decision of Ovarian Surface Epithelial Stem Cells to Undergo Neo-Oogenesis or Ovarian Tumorigenesis. *Cell Physiol Biochem* **2018**, *50*, 214-232, doi:10.1159/000494001.
15. Krzyszczyk, P.; Schloss, R.; Palmer, A.; Berthiaume, F. The Role of Macrophages in Acute and Chronic Wound Healing and Interventions to Promote Pro-wound Healing Phenotypes. *Front Physiol* **2018**, *9*, 419, doi:10.3389/fphys.2018.00419.
16. Gurtner, G.C.; Werner, S.; Barrandon, Y.; Longaker, M.T. Wound repair and regeneration. *Nature* **2008**, *453*, 314-321, doi:10.1038/nature07039.
17. Hassanshahi, A.; Moradzad, M.; Ghalamkari, S.; Fadaei, M.; Cowin, A.J.; Hassanshahi, M. Macrophage-Mediated Inflammation in Skin Wound Healing. *Cells* **2022**, *11*, doi:10.3390/cells11192953.
18. Foley, K.G.; Pritchard, M.T.; Duncan, F.E. Macrophage-derived multinucleated giant cells: hallmarks of the aging ovary. *Reproduction* **2021**, *161*, V5-V9, doi:10.1530/REP-20-0489.
19. Carter, L.E.; Cook, D.P.; Collins, O.; Gamwell, L.F.; Dempster, H.A.; Wong, H.W.; McCloskey, C.W.; Garson, K.; Vuong, N.H.; Vanderhyden, B.C. COX2 is induced in the ovarian epithelium during ovulatory wound repair and promotes cell survivaldagger. *Biol Reprod* **2019**, *101*, 961-974, doi:10.1093/biolre/ioz134.
20. Alberts B, J.A., Lewis J, et al. . *Molecular Biology of the Cell.*, 4th edition ed.; Science, N.Y.G., Ed.; New York: Garland Science.

21. Demaria, M.; Ohtani, N.; Youssef, S.A.; Rodier, F.; Toussaint, W.; Mitchell, J.R.; Laberge, R.M.; Vijg, J.; Van Steeg, H.; Dolle, M.E.; et al. An essential role for senescent cells in optimal wound healing through secretion of PDGF-AA. *Dev Cell* **2014**, *31*, 722-733, doi:10.1016/j.devcel.2014.11.012.
22. Peng, Z.; Wang, C.X.; Fang, E.H.; Wang, G.B.; Tong, Q. Role of epithelial-mesenchymal transition in gastric cancer initiation and progression. *World J Gastroenterol* **2014**, *20*, 5403-5410, doi:10.3748/wjg.v20.i18.5403.
23. Savagner, P. The epithelial-mesenchymal transition (EMT) phenomenon. *Ann Oncol* **2010**, *21 Suppl 7*, vii89-92, doi:10.1093/annonc/mdq292.
24. Sakowska, J.; Arcimowicz, L.; Jankowiak, M.; Papak, I.; Markiewicz, A.; Dziubek, K.; Kurkowiak, M.; Kote, S.; Kazmierczak-Siedlecka, K.; Polom, K.; et al. Autoimmunity and Cancer-Two Sides of the Same Coin. *Front Immunol* **2022**, *13*, 793234, doi:10.3389/fimmu.2022.793234.
25. Fan, L.; Lei, H.; Zhang, S.; Peng, Y.; Fu, C.; Shu, G.; Yin, G. Non-canonical signaling pathway of SNAI2 induces EMT in ovarian cancer cells by suppressing miR-222-3p transcription and upregulating PDCD10. *Theranostics* **2020**, *10*, 5895-5913, doi:10.7150/thno.43198.
26. Zhou, F.; Shi, L.B.; Zhang, S.Y. Ovarian Fibrosis: A Phenomenon of Concern. *Chin Med J (Engl)* **2017**, *130*, 365-371, doi:10.4103/0366-6999.198931.
27. Zavatta, A.; Parisi, F.; Mando, C.; Scaccabarozzi, C.; Savasi, V.M.; Cetin, I. Role of Inflammaging on the Reproductive Function and Pregnancy. *Clin Rev Allergy Immunol* **2023**, *64*, 145-160, doi:10.1007/s12016-021-08907-9.
28. Briley, S.M.; Jasti, S.; McCracken, J.M.; Hornick, J.E.; Fegley, B.; Pritchard, M.T.; Duncan, F.E. Reproductive age-associated fibrosis in the stroma of the mammalian ovary. *Reproduction* **2016**, *152*, 245-260, doi:10.1530/REP-16-0129.
29. Tang, M.; Zhao, M.; Shi, Y. New insight into the role of macrophages in ovarian function and ovarian aging. *Front Endocrinol (Lausanne)* **2023**, *14*, 1282658, doi:10.3389/fendo.2023.1282658.
30. Timoteo-Ferreira, F.; Mendes, S.; Rocha, N.A.; Matos, L.; Rodrigues, A.R.; Almeida, H.; Silva, E. Apocynin Dietary Supplementation Delays Mouse Ovarian Ageing. *Oxid Med Cell Longev* **2019**, *2019*, 5316984, doi:10.1155/2019/5316984.
31. Lliberos, C.; Liew, S.H.; Zareie, P.; La Gruta, N.L.; Mansell, A.; Hutt, K. Evaluation of inflammation and follicle depletion during ovarian ageing in mice. *Sci Rep* **2021**, *11*, 278, doi:10.1038/s41598-020-79488-4.
32. Ben Yaakov, T.; Wasserman, T.; Aknin, E.; Savir, Y. Single-cell analysis of the aged ovarian immune system reveals a shift towards adaptive immunity and attenuated cell function. *Elife* **2023**, *12*, doi:10.7554/eLife.74915.
33. Givan, A.L.; White, H.D.; Stern, J.E.; Colby, E.; Gosselin, E.J.; Guyre, P.M.; Wira, C.R. Flow cytometric analysis of leukocytes in the human female reproductive tract: comparison of fallopian tube, uterus, cervix, and vagina. *Am J Reprod Immunol* **1997**, *38*, 350-359, doi:10.1111/j.1600-0897.1997.tb00311.x.
34. Lee, S.K.; Kim, C.J.; Kim, D.J.; Kang, J.H. Immune cells in the female reproductive tract. *Immune Netw* **2015**, *15*, 16-26, doi:10.4110/in.2015.15.1.16.
35. Isola, J.V.V.; Ocanas, S.R.; Hubbart, C.R.; Ko, S.; Mondal, S.A.; Hense, J.D.; Schneider, A.; Kovats, S.; Freeman, W.M.; Stout, M.B. A single-cell atlas of the aging murine ovary. *bioRxiv* **2023**, doi:10.1101/2023.04.29.538828.
36. Mitchem, J.B.; Brennan, D.J.; Knolhoff, B.L.; Belt, B.A.; Zhu, Y.; Sanford, D.E.; Belaygorod, L.; Carpenter, D.; Collins, L.; Piwnica-Worms, D.; et al. Targeting tumor-infiltrating macrophages decreases tumor-initiating cells, relieves immunosuppression, and improves chemotherapeutic responses. *Cancer Res* **2013**, *73*, 1128-1141, doi:10.1158/0008-5472.CAN-12-2731.
37. Penn, C.A.; Yang, K.; Zong, H.; Lim, J.Y.; Cole, A.; Yang, D.; Baker, J.; Goonewardena, S.N.; Buckanovich, R.J. Therapeutic Impact of Nanoparticle Therapy Targeting Tumor-Associated Macrophages. *Mol Cancer Ther* **2018**, *17*, 96-106, doi:10.1158/1535-7163.MCT-17-0688.

38. Fair, T. The contribution of the maternal immune system to the establishment of pregnancy in cattle. *Front Immunol* **2015**, *6*, 7, doi:10.3389/fimmu.2015.00007.
39. Oakley, O.R.; Kim, H.; El-Amouri, I.; Lin, P.C.; Cho, J.; Bani-Ahmad, M.; Ko, C. Periovulatory leukocyte infiltration in the rat ovary. *Endocrinology* **2010**, *151*, 4551-4559, doi:10.1210/en.2009-1444.
40. McComb, S.; Thiriot, A.; Akache, B.; Krishnan, L.; Stark, F. Introduction to the Immune System. *Methods Mol Biol* **2019**, *2024*, 1-24, doi:10.1007/978-1-4939-9597-4_1.
41. Wu, R.; Van der Hoek, K.H.; Ryan, N.K.; Norman, R.J.; Robker, R.L. Macrophage contributions to ovarian function. *Hum Reprod Update* **2004**, *10*, 119-133, doi:10.1093/humupd/dmh011.
42. Henes, M.; Froeschlin, J.; Taran, F.A.; Brucker, S.; Rall, K.K.; Xenitidis, T.; Igney-Oertel, A.; Lawrenz, B.; Henes, J.C. Ovarian reserve alterations in premenopausal women with chronic inflammatory rheumatic diseases: impact of rheumatoid arthritis, Behcet's disease and spondyloarthritis on anti-Mullerian hormone levels. *Rheumatology (Oxford)* **2015**, *54*, 1709-1712, doi:10.1093/rheumatology/kev124.
43. Weiss, G.; Goldsmith, L.T.; Taylor, R.N.; Bellet, D.; Taylor, H.S. Inflammation in reproductive disorders. *Reprod Sci* **2009**, *16*, 216-229, doi:10.1177/1933719108330087.
44. Cohen-Fredarow, A.; Tadmor, A.; Raz, T.; Meterani, N.; Addadi, Y.; Nevo, N.; Solomonov, I.; Sagi, I.; Mor, G.; Neeman, M.; et al. Ovarian dendritic cells act as a double-edged pro-ovulatory and anti-inflammatory sword. *Mol Endocrinol* **2014**, *28*, 1039-1054, doi:10.1210/me.2013-1400.
45. Orisaka, M.; Mizutani, T.; Miyazaki, Y.; Shirafuji, A.; Tamamura, C.; Fujita, M.; Tsuyoshi, H.; Yoshida, Y. Chronic low-grade inflammation and ovarian dysfunction in women with polycystic ovarian syndrome, endometriosis, and aging. *Front Endocrinol (Lausanne)* **2023**, *14*, 1324429, doi:10.3389/fendo.2023.1324429.
46. Marina Martinić Kavur, G.L., Marija Pezer. *Systems Glycobiology: Immunoglobulin G Glycans as Biomarkers and Functional Effectors in Aging and Diseases*, Second Edition ed.; Barchi, J.J., Ed.; Elsevier: Volume Comprehensive Glycoscience.
47. Li, X.; Li, C.; Zhang, W.; Wang, Y.; Qian, P.; Huang, H. Inflammation and aging: signaling pathways and intervention therapies. *Signal Transduct Target Ther* **2023**, *8*, 239, doi:10.1038/s41392-023-01502-8.
48. Sousa-Victor, P.; Gutarra, S.; Garcia-Prat, L.; Rodriguez-Ubreva, J.; Ortet, L.; Ruiz-Bonilla, V.; Jardi, M.; Ballestar, E.; Gonzalez, S.; Serrano, A.L.; et al. Geriatric muscle stem cells switch reversible quiescence into senescence. *Nature* **2014**, *506*, 316-321, doi:10.1038/nature13013.
49. van Deursen, J.M. The role of senescent cells in ageing. *Nature* **2014**, *509*, 439-446, doi:10.1038/nature13193.
50. Coppe, J.P.; Patil, C.K.; Rodier, F.; Sun, Y.; Munoz, D.P.; Goldstein, J.; Nelson, P.S.; Desprez, P.Y.; Campisi, J. Senescence-associated secretory phenotypes reveal cell-nonautonomous functions of oncogenic RAS and the p53 tumor suppressor. *PLoS Biol* **2008**, *6*, 2853-2868, doi:10.1371/journal.pbio.0060301.
51. Weng, Z.; Wang, Y.; Ouchi, T.; Liu, H.; Qiao, X.; Wu, C.; Zhao, Z.; Li, L.; Li, B. Mesenchymal Stem/Stromal Cell Senescence: Hallmarks, Mechanisms, and Combating Strategies. *Stem Cells Transl Med* **2022**, *11*, 356-371, doi:10.1093/stcltm/szac004.
52. Ferrucci, L.; Fabbri, E. Inflammageing: chronic inflammation in ageing, cardiovascular disease, and frailty. *Nat Rev Cardiol* **2018**, *15*, 505-522, doi:10.1038/s41569-018-0064-2.
53. Franceschi, C.; Campisi, J. Chronic inflammation (inflammaging) and its potential contribution to age-associated diseases. *J Gerontol A Biol Sci Med Sci* **2014**, *69 Suppl 1*, S4-9, doi:10.1093/gerona/glu057.
54. Zhang, Z.; Schlamp, F.; Huang, L.; Clark, H.; Brayboy, L. Inflammaging is associated with shifted macrophage ontogeny and polarization in the aging mouse ovary. *Reproduction* **2020**, *159*, 325-337, doi:10.1530/REP-19-0330.

55. Matos, L.; Stevenson, D.; Gomes, F.; Silva-Carvalho, J.L.; Almeida, H. Superoxide dismutase expression in human cumulus oophorus cells. *Mol Hum Reprod* **2009**, *15*, 411-419, doi:10.1093/molehr/gap034.
56. Timoteo-Ferreira, F.; Abreu, D.; Mendes, S.; Matos, L.; Rodrigues, A.R.; Almeida, H.; Silva, E. Redox imbalance in age-related ovarian dysfunction and perspectives for its prevention. *Ageing Res Rev* **2021**, *68*, 101345, doi:10.1016/j.arr.2021.101345.
57. Helming, L.; Gordon, S. Molecular mediators of macrophage fusion. *Trends Cell Biol* **2009**, *19*, 514-522, doi:10.1016/j.tcb.2009.07.005.
58. Hazra, S.; Kalyan Dinda, S.; Kumar Mondal, N.; Hossain, S.R.; Datta, P.; Yasmin Mondal, A.; Malakar, P.; Manna, D. Giant cells: multiple cells unite to survive. *Front Cell Infect Microbiol* **2023**, *13*, 1220589, doi:10.3389/fcimb.2023.1220589.
59. Manjunath, Y.; Porciani, D.; Mitchem, J.B.; Suvilesh, K.N.; Avella, D.M.; Kimchi, E.T.; Staveley-O'Carroll, K.F.; Burke, D.H.; Li, G.; Kaifi, J.T. Tumor-Cell-Macrophage Fusion Cells as Liquid Biomarkers and Tumor Enhancers in Cancer. *Int J Mol Sci* **2020**, *21*, doi:10.3390/ijms21051872.
60. Vignery, A. Osteoclasts and giant cells: macrophage-macrophage fusion mechanism. *Int J Exp Pathol* **2000**, *81*, 291-304, doi:10.1111/j.1365-2613.2000.00164.x.
61. Chambers, T.J. Multinucleate giant cells. *J Pathol* **1978**, *126*, 125-148, doi:10.1002/path.1711260302.
62. Hall, B.M.; Balan, V.; Gleiberman, A.S.; Strom, E.; Krasnov, P.; Virtuoso, L.P.; Rydkina, E.; Vujcic, S.; Balan, K.; Gitlin, II; et al. p16(Ink4a) and senescence-associated beta-galactosidase can be induced in macrophages as part of a reversible response to physiological stimuli. *Aging (Albany NY)* **2017**, *9*, 1867-1884, doi:10.18632/aging.101268.
63. Milde, R.; Ritter, J.; Tennent, G.A.; Loesch, A.; Martinez, F.O.; Gordon, S.; Pepys, M.B.; Verschoor, A.; Helming, L. Multinucleated Giant Cells Are Specialized for Complement-Mediated Phagocytosis and Large Target Destruction. *Cell Rep* **2015**, *13*, 1937-1948, doi:10.1016/j.celrep.2015.10.065.
64. Matos, L.; Gouveia, A.; Almeida, H. Copper ability to induce premature senescence in human fibroblasts. *Age (Dordr)* **2012**, *34*, 783-794, doi:10.1007/s11357-011-9276-7.
65. Davalos, A.R.; Kawahara, M.; Malhotra, G.K.; Schaum, N.; Huang, J.; Ved, U.; Beausejour, C.M.; Coppe, J.P.; Rodier, F.; Campisi, J. p53-dependent release of Alarmin HMGB1 is a central mediator of senescent phenotypes. *J Cell Biol* **2013**, *201*, 613-629, doi:10.1083/jcb.201206006.
66. Dimri, G.P.; Lee, X.; Basile, G.; Acosta, M.; Scott, G.; Roskelley, C.; Medrano, E.E.; Linskens, M.; Rubelj, I.; Pereira-Smith, O.; et al. A biomarker that identifies senescent human cells in culture and in aging skin in vivo. *Proc Natl Acad Sci U S A* **1995**, *92*, 9363-9367, doi:10.1073/pnas.92.20.9363.
67. Hall, B.M.; Balan, V.; Gleiberman, A.S.; Strom, E.; Krasnov, P.; Virtuoso, L.P.; Rydkina, E.; Vujcic, S.; Balan, K.; Gitlin, I.; et al. Aging of mice is associated with p16(Ink4a)- and beta-galactosidase-positive macrophage accumulation that can be induced in young mice by senescent cells. *Aging (Albany NY)* **2016**, *8*, 1294-1315, doi:10.18632/aging.100991.
68. Ansere, V.A.; Ali-Mondal, S.; Sathiaseelan, R.; Garcia, D.N.; Isola, J.V.V.; Henseb, J.D.; Saccon, T.D.; Ocanas, S.R.; Tooley, K.B.; Stout, M.B.; et al. Cellular hallmarks of aging emerge in the ovary prior to primordial follicle depletion. *Mech Ageing Dev* **2021**, *194*, 111425, doi:10.1016/j.mad.2020.111425.
69. Liu, R.M. Aging, Cellular Senescence, and Alzheimer's Disease. *Int J Mol Sci* **2022**, *23*, doi:10.3390/ijms23041989.
70. Rossi, C.; Venturin, M.; Gubala, J.; Frasca, A.; Corsini, A.; Battaglia, C.; Bellosta, S. PURPL and NEAT1 Long Non-Coding RNAs Are Modulated in Vascular Smooth Muscle Cell Replicative Senescence. *Biomedicines* **2023**, *11*, doi:10.3390/biomedicines11123228.

71. Zhang, X.; Englund, D.A.; Aversa, Z.; Jachim, S.K.; White, T.A.; LeBrasseur, N.K. Exercise Counters the Age-Related Accumulation of Senescent Cells. *Exerc Sport Sci Rev* **2022**, *50*, 213-221, doi:10.1249/JES.0000000000000302.
72. Wiley, C.D.; Velarde, M.C.; Lecot, P.; Liu, S.; Sarnoski, E.A.; Freund, A.; Shirakawa, K.; Lim, H.W.; Davis, S.S.; Ramanathan, A.; et al. Mitochondrial Dysfunction Induces Senescence with a Distinct Secretory Phenotype. *Cell Metab* **2016**, *23*, 303-314, doi:10.1016/j.cmet.2015.11.011.
73. Montenegro, L.; Magalhaes, P.; Guerreiro, A.C.; Brandao, C.; Pinto, A.; Almeida, H.; Martins-Bessa, A.; Silva, E. The Contribution of the Sheep and the Goat Model to the Study of Ovarian Ageing. *Biology (Basel)* **2023**, *12*, doi:10.3390/biology12020270.
74. Salmonowicz, H.; Passos, J.F. Detecting senescence: a new method for an old pigment. *Aging Cell* **2017**, *16*, 432-434, doi:10.1111/acel.12580.
75. Hernandez-Pando, R.; Bornstein, Q.L.; Aguilar Leon, D.; Orozco, E.H.; Madrigal, V.K.; Martinez Cordero, E. Inflammatory cytokine production by immunological and foreign body multinucleated giant cells. *Immunology* **2000**, *100*, 352-358, doi:10.1046/j.1365-2567.2000.00025.x.
76. Coppe, J.P.; Desprez, P.Y.; Krtolica, A.; Campisi, J. The senescence-associated secretory phenotype: the dark side of tumor suppression. *Annu Rev Pathol* **2010**, *5*, 99-118, doi:10.1146/annurev-pathol-121808-102144.
77. Hou, Y.; Dan, X.; Babbar, M.; Wei, Y.; Hasselbalch, S.G.; Croteau, D.L.; Bohr, V.A. Ageing as a risk factor for neurodegenerative disease. *Nat Rev Neurol* **2019**, *15*, 565-581, doi:10.1038/s41582-019-0244-7.
78. Rodgers, J.L.; Jones, J.; Bolleddu, S.I.; Vanthenapalli, S.; Rodgers, L.E.; Shah, K.; Karia, K.; Panguluri, S.K. Cardiovascular Risks Associated with Gender and Aging. *J Cardiovasc Dev Dis* **2019**, *6*, doi:10.3390/jcdd6020019.
79. Lopez-Otin, C.; Blasco, M.A.; Partridge, L.; Serrano, M.; Kroemer, G. The hallmarks of aging. *Cell* **2013**, *153*, 1194-1217, doi:10.1016/j.cell.2013.05.039.
80. Hernandez-Segura, A.; Nehme, J.; Demaria, M. Hallmarks of Cellular Senescence. *Trends Cell Biol* **2018**, *28*, 436-453, doi:10.1016/j.tcb.2018.02.001.
81. Leonardi, G.C.; Accardi, G.; Monastero, R.; Nicoletti, F.; Libra, M. Ageing: from inflammation to cancer. *Immun Ageing* **2018**, *15*, 1, doi:10.1186/s12979-017-0112-5.
82. Nelson, S.M.; Telfer, E.E.; Anderson, R.A. The ageing ovary and uterus: new biological insights. *Hum Reprod Update* **2013**, *19*, 67-83, doi:10.1093/humupd/dms043.
83. Recognizing the importance of ovarian aging research. *Nat Aging* **2022**, *2*, 1071-1072, doi:10.1038/s43587-022-00339-0.
84. Giatromanolaki, A.; Kouroupi, M.; Balaska, K.; Koukourakis, M.I. A Novel Lipofuscin-detecting Marker of Senescence Relates With Hypoxia, Dysregulated Autophagy and With Poor Prognosis in Non-small-cell-lung Cancer. *In Vivo* **2020**, *34*, 3187-3193, doi:10.21873/invivo.12154.
85. Varghese, A.; Lele, S. Rare Ovarian Tumors. In *Ovarian Cancer*, Lele, S., Ed.; Brisbane (AU), 2022.
86. Blagosklonny, M.V. Rapamycin-induced glucose intolerance: hunger or starvation diabetes. *Cell Cycle* **2011**, *10*, 4217-4224, doi:10.4161/cc.10.24.18595.
87. Laberge, R.M.; Sun, Y.; Orjalo, A.V.; Patil, C.K.; Freund, A.; Zhou, L.; Curran, S.C.; Davalos, A.R.; Wilson-Edell, K.A.; Liu, S.; et al. MTOR regulates the pro-tumorigenic senescence-associated secretory phenotype by promoting IL1A translation. *Nat Cell Biol* **2015**, *17*, 1049-1061, doi:10.1038/ncb3195.
88. Coussens, L.M.; Werb, Z. Inflammation and cancer. *Nature* **2002**, *420*, 860-867, doi:10.1038/nature01322.
89. Zhu, X.; Chen, Z.; Shen, W.; Huang, G.; Sedivy, J.M.; Wang, H.; Ju, Z. Inflammation, epigenetics, and metabolism converge to cell senescence and ageing: the regulation and intervention. *Signal Transduct Target Ther* **2021**, *6*, 245, doi:10.1038/s41392-021-00646-9.

90. Faget, D.V.; Ren, Q.; Stewart, S.A. Unmasking senescence: context-dependent effects of SASP in cancer. *Nat Rev Cancer* **2019**, *19*, 439-453, doi:10.1038/s41568-019-0156-2.
91. Korbecki, J.; Siminska, D.; Gassowska-Dobrowolska, M.; Listos, J.; Gutowska, I.; Chlubek, D.; Baranowska-Bosiacka, I. Chronic and Cycling Hypoxia: Drivers of Cancer Chronic Inflammation through HIF-1 and NF-kappaB Activation: A Review of the Molecular Mechanisms. *Int J Mol Sci* **2021**, *22*, doi:10.3390/ijms221910701.
92. Iyengar, N.M.; Gucalp, A.; Dannenberg, A.J.; Hudis, C.A. Obesity and Cancer Mechanisms: Tumor Microenvironment and Inflammation. *J Clin Oncol* **2016**, *34*, 4270-4276, doi:10.1200/JCO.2016.67.4283.
93. Purdie, D.M.; Bain, C.J.; Siskind, V.; Webb, P.M.; Green, A.C. Ovulation and risk of epithelial ovarian cancer. *Int J Cancer* **2003**, *104*, 228-232, doi:10.1002/ijc.10927.
94. Zhang, Y.; Luo, G.; Li, M.; Guo, P.; Xiao, Y.; Ji, H.; Hao, Y. Global patterns and trends in ovarian cancer incidence: age, period and birth cohort analysis. *BMC Cancer* **2019**, *19*, 984, doi:10.1186/s12885-019-6139-6.
95. Bernal, A.; Mendez-Moran, L.; Fajardo-Gutierrez, A.; Gonzalez-Lira, G.; Escudero, P.; Ortiz, H. Univariate and multivariate analysis of risk factors for ovarian cancer: case-control study, Mexico City. *Arch Med Res* **1995**, *26*, 245-249.
96. Pollack, A.Z.; Rivers, K.; Ahrens, K.A. Parity associated with telomere length among US reproductive age women. *Hum Reprod* **2018**, *33*, 736-744, doi:10.1093/humrep/dey024.
97. Choi, P.W.; Yang, J.; Ng, S.K.; Feltmate, C.; Muto, M.G.; Hasselblatt, K.; Lafferty-Whyte, K.; JeBailey, L.; MacConaill, L.; Welch, W.R.; et al. Loss of E-cadherin disrupts ovarian epithelial inclusion cyst formation and collective cell movement in ovarian cancer cells. *Oncotarget* **2016**, *7*, 4110-4121, doi:10.18632/oncotarget.6588.
98. Scully, R.E. Pathology of ovarian cancer precursors. *J Cell Biochem Suppl* **1995**, *23*, 208-218, doi:10.1002/jcb.240590928.
99. Feeley, K.M.; Wells, M. Precursor lesions of ovarian epithelial malignancy. *Histopathology* **2001**, *38*, 87-95, doi:10.1046/j.1365-2559.2001.01042.x.
100. Tan, O.L.; Hurst, P.R.; Fleming, J.S. Location of inclusion cysts in mouse ovaries in relation to age, pregnancy, and total ovulation number: implications for ovarian cancer? *J Pathol* **2005**, *205*, 483-490, doi:10.1002/path.1719.
101. Elinav, E.; Nowarski, R.; Thaiss, C.A.; Hu, B.; Jin, C.; Flavell, R.A. Inflammation-induced cancer: crosstalk between tumours, immune cells and microorganisms. *Nat Rev Cancer* **2013**, *13*, 759-771, doi:10.1038/nrc3611.
102. Yuan, A.; Chen, J.J.; Yao, P.L.; Yang, P.C. The role of interleukin-8 in cancer cells and microenvironment interaction. *Front Biosci* **2005**, *10*, 853-865, doi:10.2741/1579.
103. Amargant, F.; Manuel, S.L.; Tu, Q.; Parkes, W.S.; Rivas, F.; Zhou, L.T.; Rowley, J.E.; Villanueva, C.E.; Hornick, J.E.; Shekhawat, G.S.; et al. Ovarian stiffness increases with age in the mammalian ovary and depends on collagen and hyaluronan matrices. *Aging Cell* **2020**, *19*, e13259, doi:10.1111/acel.13259.
104. Umehara, T.; Winstanley, Y.E.; Andreas, E.; Morimoto, A.; Williams, E.J.; Smith, K.M.; Carroll, J.; Febbraio, M.A.; Shimada, M.; Russell, D.L.; et al. Female reproductive life span is extended by targeted removal of fibrotic collagen from the mouse ovary. *Sci Adv* **2022**, *8*, eabn4564, doi:10.1126/sciadv.abn4564.
105. Anggorowati, N.; Ratna Kurniasari, C.; Damayanti, K.; Cahyanti, T.; Widodo, I.; Ghozali, A.; Romi, M.M.; Sari, D.C.; Arfian, N. Histochemical and Immunohistochemical Study of alpha-SMA, Collagen, and PCNA in Epithelial Ovarian Neoplasm. *Asian Pac J Cancer Prev* **2017**, *18*, 667-671, doi:10.22034/APJCP.2017.18.3.667.
106. Czernobilsky, B.; Shezen, E.; Lifschitz-Mercer, B.; Fogel, M.; Luzon, A.; Jacob, N.; Skalli, O.; Gabbiani, G. Alpha smooth muscle actin (alpha-SM actin) in normal human ovaries, in ovarian stromal hyperplasia and in ovarian neoplasms. *Virchows Arch B Cell Pathol Incl Mol Pathol* **1989**, *57*, 55-61, doi:10.1007/BF02899065.

107. Campisi, J. Cellular senescence as a tumor-suppressor mechanism. *Trends Cell Biol* **2001**, *11*, S27-31, doi:10.1016/s0962-8924(01)02151-1.
108. Okamura, H.; Katabuchi, H. Detailed morphology of human ovarian surface epithelium focusing on its metaplastic and neoplastic capability. *Ital J Anat Embryol* **2001**, *106*, 263-276.
109. biosystems, L. Leica biosystems: H&E Staining Overview: A Guide to Best Practices. Available online: https://www.leicabiosystems.com/knowledge-pathway/he-staining-overview-a-guide-to-best-practices/ (accessed on 2023, August).
110. Alison J. Hobro, N.I.S. *An evaluation of fixation methods: Spatial and compositional cellular changes observed by Raman imaging*; Elsevier: 2017; Volume 91.
111. Lillie, R.D.; Burtner, H.J. Stable sudanophilia of human neutrophil leucocytes in relation to peroxidase and oxidase. *J Histochem Cytochem* **1953**, *1*, 8-26, doi:10.1177/1.1.8.
112. Sheehan, H.L.; Storey, G.W. An improved method of staining leucocyte granules with Sudan black B. *J Pathol Bacteriol* **1947**, *59*, 336, doi:10.1002/path.1700590142.
113. Abcam. Immunohistochemistry (IHC): the complete guide. Available online: https://www.abcam.com/content/immunohistochemistry-the-complete-guide (accessed on
114. Bradford, M.M. A rapid and sensitive method for the quantitation of microgram quantities of protein utilizing the principle of protein-dye binding. *Anal Biochem* **1976**, *72*, 248-254, doi:10.1006/abio.1976.9999.
115. Bio-Rad Laboratories, I. Quick Start™ Bradford Protein Assay - Instruction Manual.
116. Sasamoto, N.; Stewart, P.A.; Wang, T.; Yoder, S.J.; Chellappan, S.; Hecht, J.L.; Fridley, B.L.; Terry, K.L.; Tworoger, S.S. Lifetime ovulatory years and ovarian cancer gene expression profiles. *J Ovarian Res* **2022**, *15*, 59, doi:10.1186/s13048-022-00995-1.
117. Wu, J.; Liu, Y.; Song, Y.; Wang, L.; Ai, J.; Li, K. Aging conundrum: A perspective for ovarian aging. *Front Endocrinol (Lausanne)* **2022**, *13*, 952471, doi:10.3389/fendo.2022.952471.
118. te Velde, E.R.; Pearson, P.L. The variability of female reproductive ageing. *Hum Reprod Update* **2002**, *8*, 141-154, doi:10.1093/humupd/8.2.141.
119. Kakimoto, Y.; Okada, C.; Kawabe, N.; Sasaki, A.; Tsukamoto, H.; Nagao, R.; Osawa, M. Myocardial lipofuscin accumulation in ageing and sudden cardiac death. *Sci Rep* **2019**, *9*, 3304, doi:10.1038/s41598-019-40250-0.
120. Urzua, U.; Chacon, C.; Espinoza, R.; Martinez, S.; Hernandez, N. Parity-Dependent Hemosiderin and Lipofuscin Accumulation in the Reproductively Aged Mouse Ovary. *Anal Cell Pathol (Amst)* **2018**, *2018*, 1289103, doi:10.1155/2018/1289103.
121. Evangelou, K.; Gorgoulis, V.G. Sudan Black B, The Specific Histochemical Stain for Lipofuscin: A Novel Method to Detect Senescent Cells. *Methods Mol Biol* **2017**, *1534*, 111-119, doi:10.1007/978-1-4939-6670-7_10.
122. REZNIK-SCHULLE, J.M.W.a.H. *Morphological and Histochemical Characteristics of Pigments in Aging F344 Rats*; Volume 17.
123. Vida, C.; de Toda, I.M.; Cruces, J.; Garrido, A.; Gonzalez-Sanchez, M.; De la Fuente, M. Role of macrophages in age-related oxidative stress and lipofuscin accumulation in mice. *Redox Biol* **2017**, *12*, 423-437, doi:10.1016/j.redox.2017.03.005.
124. Janeway CA Jr, T.P., Walport M, et al. *The distribution and functions of immunoglobulin isotypes.*, 5th edition ed.; 2011.
125. Kdimati, S.; Mullins, C.S.; Linnebacher, M. Cancer-Cell-Derived IgG and Its Potential Role in Tumor Development. *Int J Mol Sci* **2021**, *22*, doi:10.3390/ijms222111597.
126. Lucas, S.D.; Karlsson-Parra, A.; Nilsson, B.; Grimelius, L.; Akerstrom, G.; Rastad, J.; Juhlin, C. Tumor-specific deposition of immunoglobulin G and complement in papillary thyroid carcinoma. *Hum Pathol* **1996**, *27*, 1329-1335, doi:10.1016/s0046-8177(96)90346-9.
127. Yu, L.; Wan, Q.; Liu, Q.; Fan, Y.; Zhou, Q.; Skowronski, A.A.; Wang, S.; Shao, Z.; Liao, C.Y.; Ding, L.; et al. IgG is an aging factor that drives adipose tissue fibrosis and metabolic decline. *Cell Metab* **2024**, *36*, 793-807 e795, doi:10.1016/j.cmet.2024.01.015.

128. Lauc, G. Can we suppress chronic systemic inflammation and postpone age-related diseases by targeting the IgG glycome? *Expert Opin Ther Targets* **2023**, 1-9, doi:10.1080/14728222.2023.2277218.
129. Boshtam, M., Kouhpayeh, S., Amini, F., Azizi, Y., Najaflu, M., Shariati, L., & Khanahmad, H. . Anti-inflammatory effects of apocynin: a narrative review of the evidence. *All Life* **2021**, *14(1)*, 997–1010, doi:10.1080/26895293.2021.1990136.
130. Barbieri, S.S.; Cavalca, V.; Eligini, S.; Brambilla, M.; Caiani, A.; Tremoli, E.; Colli, S. Apocynin prevents cyclooxygenase 2 expression in human monocytes through NADPH oxidase and glutathione redox-dependent mechanisms. *Free Radic Biol Med* **2004**, *37*, 156-165, doi:10.1016/j.freeradbiomed.2004.04.020.
131. Sutti, S.; Jindal, A.; Locatelli, I.; Vacchiano, M.; Gigliotti, L.; Bozzola, C.; Albano, E. Adaptive immune responses triggered by oxidative stress contribute to hepatic inflammation in NASH. *Hepatology* **2014**, *59*, 886-897, doi:10.1002/hep.26749.
132. Duffy, D.M.; Ko, C.; Jo, M.; Brannstrom, M.; Curry, T.E. Ovulation: Parallels With Inflammatory Processes. *Endocr Rev* **2019**, *40*, 369-416, doi:10.1210/er.2018-00075.
133. Bajwa, P.; Nagendra, P.B.; Nielsen, S.; Sahoo, S.S.; Bielanowicz, A.; Lombard, J.M.; Wilkinson, J.E.; Miller, R.A.; Tanwar, P.S. Age related increase in mTOR activity contributes to the pathological changes in ovarian surface epithelium. *Oncotarget* **2016**, *7*, 19214-19227, doi:10.18632/oncotarget.8468.
134. Ahmed, N.; Thompson, E.W.; Quinn, M.A. Epithelial-mesenchymal interconversions in normal ovarian surface epithelium and ovarian carcinomas: an exception to the norm. *J Cell Physiol* **2007**, *213*, 581-588, doi:10.1002/jcp.21240.
135. Wu, C.; Xu, B.; Li, X.; Ma, W.; Zhang, P.; Chen, X.; Wu, J. Tracing and Characterizing the Development of Transplanted Female Germline Stem Cells In Vivo. *Mol Ther* **2017**, *25*, 1408-1419, doi:10.1016/j.ymthe.2017.04.019.
136. Jin, H.; Yu, Y.; Zhang, T.; Zhou, X.; Zhou, J.; Jia, L.; Wu, Y.; Zhou, B.P.; Feng, Y. Snail is critical for tumor growth and metastasis of ovarian carcinoma. *Int J Cancer* **2010**, *126*, 2102-2111, doi:10.1002/ijc.24901.
137. Iwatsuki, M.; Mimori, K.; Yokobori, T.; Ishi, H.; Beppu, T.; Nakamori, S.; Baba, H.; Mori, M. Epithelial-mesenchymal transition in cancer development and its clinical significance. *Cancer Sci* **2010**, *101*, 293-299, doi:10.1111/j.1349-7006.2009.01419.x.
138. Wijshake, T.; Zou, Z.; Chen, B.; Zhong, L.; Xiao, G.; Xie, Y.; Doench, J.G.; Bennett, L.; Levine, B. Tumor-suppressor function of Beclin 1 in breast cancer cells requires E-cadherin. *Proc Natl Acad Sci U S A* **2021**, *118*, doi:10.1073/pnas.2020478118.
139. Werness, B.A.; Afify, A.M.; Bielat, K.L.; Eltabbakh, G.H.; Piver, M.S.; Paterson, J.M. Altered surface and cyst epithelium of ovaries removed prophylactically from women with a family history of ovarian cancer. *Hum Pathol* **1999**, *30*, 151-157, doi:10.1016/s0046-8177(99)90269-1.
140. Sherman, M.E.; Lee, J.S.; Burks, R.T.; Struewing, J.P.; Kurman, R.J.; Hartge, P. Histopathologic features of ovaries at increased risk for carcinoma. A case-control analysis. *Int J Gynecol Pathol* **1999**, *18*, 151-157, doi:10.1097/00004347-199904000-00009.
141. Salazar, H.; Godwin, A.K.; Daly, M.B.; Laub, P.B.; Hogan, W.M.; Rosenblum, N.; Boente, M.P.; Lynch, H.T.; Hamilton, T.C. Microscopic benign and invasive malignant neoplasms and a cancer-prone phenotype in prophylactic oophorectomies. *J Natl Cancer Inst* **1996**, *88*, 1810-1820, doi:10.1093/jnci/88.24.1810.
142. Auersperg, N.; Wong, A.S.; Choi, K.C.; Kang, S.K.; Leung, P.C. Ovarian surface epithelium: biology, endocrinology, and pathology. *Endocr Rev* **2001**, *22*, 255-288, doi:10.1210/edrv.22.2.0422.
143. Flesken-Nikitin, A.; Choi, K.C.; Eng, J.P.; Shmidt, E.N.; Nikitin, A.Y. Induction of carcinogenesis by concurrent inactivation of p53 and Rb1 in the mouse ovarian surface epithelium. *Cancer Res* **2003**, *63*, 3459-3463.

144. Wu, R.; Hendrix-Lucas, N.; Kuick, R.; Zhai, Y.; Schwartz, D.R.; Akyol, A.; Hanash, S.; Misek, D.E.; Katabuchi, H.; Williams, B.O.; et al. Mouse model of human ovarian endometrioid adenocarcinoma based on somatic defects in the Wnt/beta-catenin and PI3K/Pten signaling pathways. *Cancer Cell* **2007**, *11*, 321-333, doi:10.1016/j.ccr.2007.02.016.
145. Dinulescu, D.M.; Ince, T.A.; Quade, B.J.; Shafer, S.A.; Crowley, D.; Jacks, T. Role of K-ras and Pten in the development of mouse models of endometriosis and endometrioid ovarian cancer. *Nat Med* **2005**, *11*, 63-70, doi:10.1038/nm1173.
146. Wynn, T.A.; Vannella, K.M. Macrophages in Tissue Repair, Regeneration, and Fibrosis. *Immunity* **2016**, *44*, 450-462, doi:10.1016/j.immuni.2016.02.015.
147. Martinez, F.O.; Helming, L.; Gordon, S. Alternative activation of macrophages: an immunologic functional perspective. *Annu Rev Immunol* **2009**, *27*, 451-483, doi:10.1146/annurev.immunol.021908.132532.
148. Isola, J.V.V.; Ocanas, S.R.; Hubbart, C.R.; Ko, S.; Mondal, S.A.; Hense, J.D.; Carter, H.N.C.; Schneider, A.; Kovats, S.; Alberola-Ila, J.; et al. A single-cell atlas of the aging murine ovary. *bioRxiv* **2023**, doi:10.1101/2023.04.29.538828.
149. Koyuncu, S.; Loureiro, R.; Lee, H.J.; Wagle, P.; Krueger, M.; Vilchez, D. Rewiring of the ubiquitinated proteome determines ageing in C. elegans. *Nature* **2021**, *596*, 285-290, doi:10.1038/s41586-021-03781-z.
150. Chang, C.L. Facilitation of Ovarian Response by Mechanical Force-Latest Insight on Fertility Improvement in Women with Poor Ovarian Response or Primary Ovarian Insufficiency. *Int J Mol Sci* **2023**, *24*, doi:10.3390/ijms241914751.
151. Fathalla, M.F. Incessant ovulation--a factor in ovarian neoplasia? *Lancet* **1971**, *2*, 163, doi:10.1016/s0140-6736(71)92335-x.
152. Fathalla, M.F. Non-hormonal interruption of incessant ovulation as a potential approach for ovarian cancer prevention. *Int J Gynaecol Obstet* **2016**, *132*, 356-358, doi:10.1016/j.ijgo.2015.11.006.
153. Yan, F.; Zhao, Q.; Li, Y.; Zheng, Z.; Kong, X.; Shu, C.; Liu, Y.; Shi, Y. The role of oxidative stress in ovarian aging: a review. *J Ovarian Res* **2022**, *15*, 100, doi:10.1186/s13048-022-01032-x.
154. Isono, W.; Wada-Hiraike, O.; Kawamura, Y.; Fujii, T.; Osuga, Y.; Kurihara, H. Administration of Oral Contraceptives Could Alleviate Age-Related Fertility Decline Possibly by Preventing Ovarian Damage in a Mouse Model. *Reprod Sci* **2018**, *25*, 1413-1423, doi:10.1177/1933719117746758.
155. Miyamoto, K.; Sato, E.F.; Kasahara, E.; Jikumaru, M.; Hiramoto, K.; Tabata, H.; Katsuragi, M.; Odo, S.; Utsumi, K.; Inoue, M. Effect of oxidative stress during repeated ovulation on the structure and functions of the ovary, oocytes, and their mitochondria. *Free Radic Biol Med* **2010**, *49*, 674-681, doi:10.1016/j.freeradbiomed.2010.05.025.
156. Zhang, P.; Zhang, P.; Shi, B.; Zhou, M.; Jiang, H.; Zhang, H.; Pan, X.; Gao, H.; Sun, H.; Li, Z. Galectin-1 overexpression promotes progression and chemoresistance to cisplatin in epithelial ovarian cancer. *Cell Death Dis* **2014**, *5*, e991, doi:10.1038/cddis.2013.526.
157. Zhu, J.; Zheng, Y.; Zhang, H.; Liu, Y.; Sun, H.; Zhang, P. Galectin-1 induces metastasis and epithelial-mesenchymal transition (EMT) in human ovarian cancer cells via activation of the MAPK JNK/p38 signalling pathway. *Am J Transl Res* **2019**, *11*, 3862-3878.